

1

Dependence Discovery from Multimodal Data via 2 Multiscale Graph Correlation

3 Cencheng Shen¹, Carey E. Priebe², Mauro Maggioni³, and Joshua T. Vogelstein*⁴

4 ¹Department of Statistics, Temple University

5 ²Department of Applied Mathematics and Statistics, Johns Hopkins University

6 ²Department of Mathematics, Duke University

7 ⁴Department of Biomedical Engineering and Institute for Computational Medicine, Johns
8 Hopkins University

9 June 23, 2016

10

Abstract

11 Understanding and discovering dependence between multiple properties or measurements
12 is a fundamental task not just in science, but also policy, commerce, and other domains. An
13 ideal test for dependence would have the following properties: (1) Theoretical consistency such
14 that the testing power converges to 1 under any dependency structure and dimensionality. (2)
15 Strong empirical performance on a wide variety of low- and high-dimensional simulations. (3)
16 Provides insight into the nature of the dependence, rather than merely a valid p-value. (4)
17 On real data, detects dependence when it exists, and does not detect dependence when it
18 does not exist. No existing test satisfies all of these properties. In this paper we propose a
19 novel dependence test statistic called “Multiscale Graph Correlation” (Mgc), by combining the
20 ideas of distance correlation with nearest-neighbor testing. More specifically, we only use the
21 distance correlations amongst the nearest-neighbors of each data point, yielding a sparse,
22 and therefore regularized, matrix from which we can compute the test statistic. We demon-
23 strate that Mgc has all of the above properties via a series of theoretical proofs, numerical
24 simulations, and real data experiments. Specifically, we applied Mgc in several real applica-
25 tions: (i) detect dependence between brain disorder and hippocampus shape, (ii) determine
26 whether either of two pipelines can detect dependence between brain activity and personality,
27 and (iii) do not inflate non-existent dependence between resting activity and a spurious stim-
28 ulation. Mgc performs as well or better than previously proposed methods in essentially all
29 theory, low-dimensional and high-dimensional simulations, and real data experiments. Mgc is
30 therefore poised to be useful in a wide variety of applications, requiring only data and a dis-
31 similarity function for both measurement types. Both MATLAB and R code are provided here:
32 <https://github.com/jovo/RankdCorr/>.

33 *Keywords:* testing independence, distance correlation, k-nearest-neighbor, local correlation coef-
34 ficient, permutation test

*jovo@jhu.edu

35 **Contents**

36	A Simulation Functions	20
37	B Supplementary Results	24
38	C Dependence Measures	27
39	C.1 (Global) MANTEL Test	27
40	C.2 (Global) Distance Correlation	28
41	C.3 (Global) Modified Distance Correlation	29
42	C.4 Multiscale Graph Correlations (Mgc)	30
43	C.5 Heller, Heller & Gorfine (HHG)	31
44	D Mgc Algorithms and Testing Procedures	31
45	D.1 Algorithms	32
46	D.2 Discussions of Optimal Scale Estimation	33
47	E Proofs	39

48 Detecting dependency among multiple data sets is one of the most important and fundamental
49 tasks in computational statistics and data science. Indeed, prior to embarking on a predictive
50 machine learning investigation, one might first check whether any dependence is detectable; if not,
51 high-quality predictions will be unlikely. The founders of statistics first highlighted the importance
52 of this task, starting with Pearson, who developed Pearson's Product-Moment Correlation statistic
53 [1]. Since then, researchers have consistently developed new and improved methods (see [2] for
54 a recent review and discussion).

55 In the era of big data, several challenges emerge as particularly prevalent and therefore, problem-
56 atic. First, the dependencies between different modalities of data can be highly **non-linear**. While
57 this has always been the case, the relative abundance of data has led to an increased demand in
58 checking for dependence in many previously uninvestigated settings. Second, the **dimensionality**
59 of individual samples is growing at exponential rates, with genomics and connectomics data, for
60 example, often accruing millions or billions of dimensions per data point. At the same time, the
61 **sample sizes** are not increasing proportionally, meaning that we often have datasets with very
62 high-dimensions and relatively low sample size. Third, the data are often **complicated**: networks,
63 shapes, questionnaires, semi-structured text are all typical examples. For example, we may de-
64 sire to understand whether brain shape and disease status are related, so that we can develop
65 prognostic biomarkers to combat the deleterious effects of degenerative neurological disorders [3].
66 Fourth, because we will often have a data deluge, with myriad different measurements, it is impor-
67 tant to be able to compute the results reasonably **efficiently**. Fifth, when working with big data,
68 statistical procedures often have hyper-parameters that require tuning. Many such procedures
69 lack any guidance in choosing the value of those hyper-parameters, thereby requiring users of the
70 procedures to concoct their own heuristics. It is desirable that a procedure is **adaptive**, in that it
71 can automatically set its hyper-parameters in a valid way. Finally, as alluded to above, checking for
72 dependence is rarely the final step in the analysis. Frequently, investigators and analysts desire
73 more than a simple p-value, rather, they desire some insight into the nature of the **dependence**
74 **structure**, which can then inform them in terms of how to proceed. We desire tests that satisfy
75 the above desiderata, both in theory as well as in extensive simulations and real data problems.

76 There are two key insights from the literature that we combine to develop our methodology that
77 satisfies the above desiderata. First, a collection of pairwise comparisons suffices to characterize
78 a joint distribution [4]. Second, nonlinear manifolds can be approximated by local linear spaces
79 [5]. Our approach, Multiscale Graph Correlation (Mgc), leverages and improves upon recent devel-

80 opments from both subdisciplines of data science.

81 Interpoint pairwise comparison matrices have been used for over 100 years for various statistical
82 purposes [4]. Perhaps one of the earliest examples of using them for dependence testing comes
83 from Karl Pearson [1], who created a special case of something subsequently called a “generalized
84 correlation coefficient” [6]. Generalized correlation coefficients start with n pairs of observations
85 (x_i, y_i) , where x ’s and y ’s both might vectors, shapes, networks, etc. And then, a comparison
86 function is defined for each. Specifically, let $a_{ij} = \delta_x(x_i, x_j)$, and let $b_{ij} = \delta_y(y_i, y_j)$. Thus, $A =$
87 $\{a_{ij}\}$ and $B = \{b_{ij}\}$ are the $n \times n$ interpoint comparison matrices for x and y , respectively. Without
88 loss of generality, assuming A and B have zero mean, a generalized correlation coefficient can
89 then be written:

$$C = \frac{1}{z} \sum_{i,j=1}^n a_{ij} b_{ij}, \quad (1)$$

90 where z is proportional to standard deviations of A and B , that is $z = n^2 \sigma_a \sigma_b$. In words, C is the
91 correlation across *pairwise comparisons*, rather than the individual data samples. C has many
92 well known special cases historically, including Pearson’s [1], Spearman’s [7], Kendall’s [6], and
93 Mantel’s correlation [8]. Recently, Szekely et al. [9] extended these approaches, letting δ_x and δ_y
94 to be the Euclidean distance, followed by subtracting the row means and column means, resulting
95 in “doubly centered” distances. Impressively, they proved that this “distance correlation” (DCORR)
96 statistic is a consistent test for independence for any joint distribution (under suitable regularity
97 conditions), that is, the DCORR’s power approaches 1 as sample size approaches infinity, for any
98 joint distribution of finite dimension and finite second moments. Szekely et al. [10] further proposed
99 a modified version called MCORR, which they prove to be consistent even as the dimensions of x
100 and y increase to infinity as well. Moreover, because these distance based tests merely require
101 a comparison function for both x and y , Lyons was able to prove that they are consistent even in
102 other metric spaces, including certain networks, shapes, and other complicated spaces [11]. Thus,
103 existing generalized correlation coefficient based tests therefore work well in high dimensions
104 and low sample sizes, including in complicated domains, and are reasonably computationally
105 efficient. But, empirically, they struggle in various non-linear settings, perhaps because they do
106 not automatically adapt to the data. Therefore, they also do provide insight into the nature of the
107 dependence.

108 A deep insight that the generalized correlation coefficient tests have yet to capitalized on, that
109 could help address the above described limitations, is that nonlinear shapes can be approximated
110 by **locally** linear ones [5]. Locality has been utilized for classification and regression [12], data

111 compression [13], and recommender systems [14], to name a few of the myriad data science
112 problems for which locality has already reaped benefits. Moreover, it has become an invaluable
113 tool in unfolding nonlinear geometry in many recent development of nonlinear embedding algo-
114 rithms, dating back to the 1950s [15], and more recently making a resurgence with the advent of
115 Isomap [16, 17], Local Linear Embedding [18, 19], and Laplacien eigenmaps [20], among many
116 others. The concept of locality, while popular within certain fields has only entered into testing very
117 infrequently [21–23]. These approaches, like the distance correlation based ones, have the advan-
118 tage of naturally operating on complicated data, because they only require a comparison function
119 between observations. They can also have strong theoretical guarantees. However, these local
120 testing approaches focus on two-sample testing, rather than dependence testing.

121 The challenge associated with all of methods that employ locality is in choosing the appropriate
122 scale (or neighborhood size) [24]. Even those approaches that do provide a mechanism for op-
123 timizing neighborhood size often do so without any theoretical guarantees, and choose based
124 on some surrogate function, rather than the exploitation task at hand. In either case, changing
125 the neighborhood size for many of these algorithms typically requires running the entire algorithm
126 again, rendering it computationally intractable. Thus, a gap remains in the literature: a depen-
127 dence test that has all of the desirable properties of the distance based tests, but also performs
128 well in highly nonlinear settings via adapting scale appropriately, thereby providing insight into the
129 most informative neighborhood sizes for both understanding and subsequent inference purposes.

130 Multiscale Graph Correlation

131 All dependence tests start from the same setting: we observe n pairs of observations (x_i, y_i) , and
132 we first desire to know whether the x 's and y 's are independent of one another, and if so, we then
133 desire to understand the nature of that dependence structure.

134 Multiscale Graph Correlation (Mgc) combines generalized correlation coefficients with locality.
135 Specifically, let $R(a_{ij})$ be the “rank” of x_i relative to x_j , that is, $R(a_{ij}) = k$ if x_i is the k^{th} clos-
136 est point (or “neighbor”) to x_j , starting from 1 to n , and define $R(b_{ij})$ equivalently for the y 's. For
137 any neighborhood size k around each x and any neighborhood size l around each y , we define

138 the rank-truncated pairwise comparisons:

$$a_{ij}^k = \begin{cases} a_{ij} - \bar{a}^k, & \text{if } R(a_{ij}) \leq k, \\ 0, & \text{otherwise;} \end{cases} \quad b_{ij}^l = \begin{cases} b_{ij} - \bar{b}^l, & \text{if } R(b_{ij}) \leq l, \\ 0, & \text{otherwise;} \end{cases} \quad (2)$$

139 where \bar{a}^k and \bar{b}^l are the local means such that $\sum_{i,j=1}^n a_{ij}^k = \sum_{i,j=1}^n b_{ij}^l = 0$. We define a *local*
140 variant of any global generalized correlation coefficient by excluding large distances:

$$C^{kl} = \frac{1}{z_{kl}} \sum_{i,j=1}^n a_{ij}^k b_{ij}^l, \quad (3)$$

141 where $z_{kl} = n^2 \sigma_a^k \sigma_b^l$, with σ_a^k and σ_b^l being the standard deviations for the truncated pairwise
142 comparisons. There are a maximum of n^2 different local correlations, one for each possible com-
143 bination of k and l (more technical details of Mgc are in Appendix C.4). Among all n^2 local statistics,
144 $\{C^{kl}\}$, Mgc selects the best local statistic for testing. Figure 1 schematically illustrates Mgc on a
145 particular nonlinear dependence structure.

146 Having defined how to compute Mgc, we face three challenges to make the method practical. First,
147 in addition to the test statistic, we need to compute the null distribution, so that we may find the
148 critical values and p-values. Second, naïvely, computing all local C^{kl} statistics would require an
149 unacceptably large computational budget. Third, having computed all local statistics, we require a
150 method for choosing the optimal neighborhood size, in such a way that the test is still consistent,
151 and not biased (so the resultant p-value remains valid).

152 Computing the p-values from the test statistic is straightforward. Specifically, we can permute the
153 labels of either the x_i 's or the y_i 's, and then compute the Mgc statistics on the permuted data
154 [25]. By permuting the labels, we have rendered the two different views of the data independent.
155 Doing so many times yields an empirical estimate of the null distribution, which we can use to
156 compute the critical value and p-value. This procedure is somewhat time consuming, which makes
157 computing the test statistics for all neighborhoods efficiently even more important.

158 Nearly all algorithms that employ regularization (for example, sparse methods, feature selection,
159 dimensionality reduction) face a similar dilemma: how to efficiently choose the hyper-parameters.
160 Most manifold learning algorithms require that the user essentially runs the entire algorithm again
161 from scratch for each different hyper-parameter setting, a pursuit that can be exponentially taxing
162 as the number of hyper-parameters increases. In our case, once the rank information is pro-
163 vided, each distance-based local correlation takes $O(n^2)$ time to compute (Pseudocode 1 in Ap-
164 pendix D.1), which means a straightforward algorithm to compute all local correlations would take

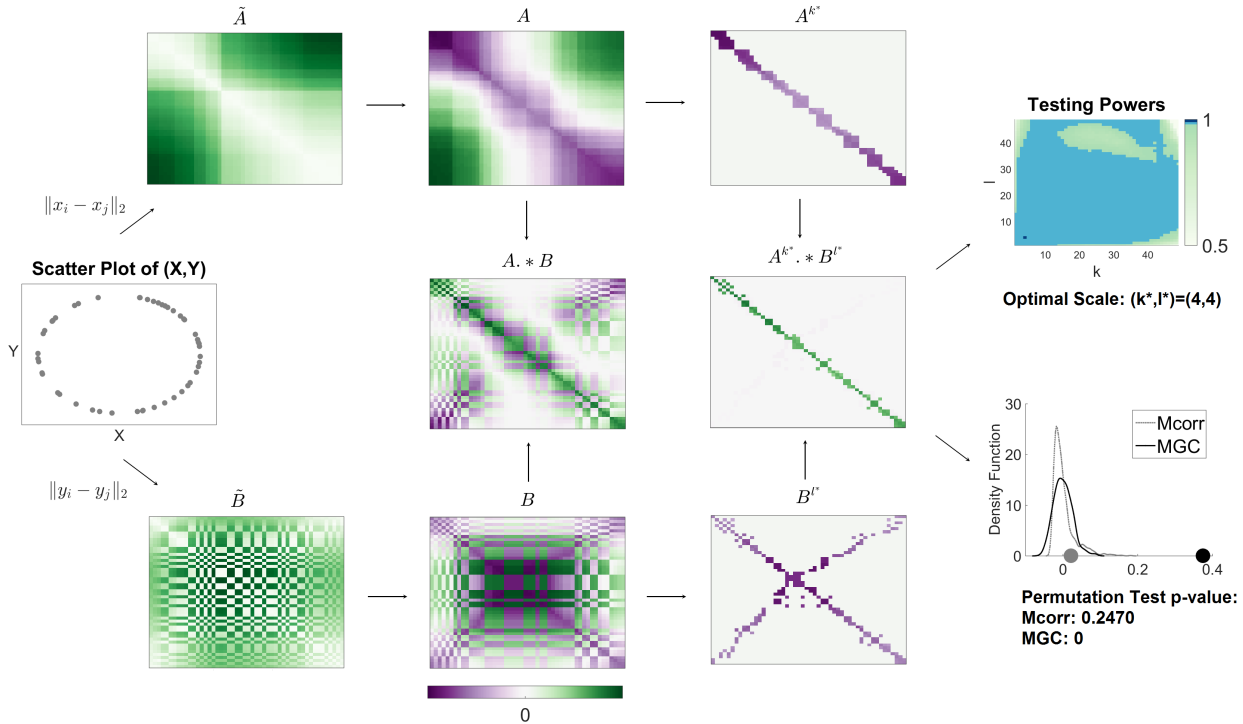


Figure 1: Flowchart for Mgc computation: Column 1: (X, Y) have a circle relationship. Column 2: The heat maps of \tilde{A} and \tilde{B} , which are the pairwise Euclidean distance matrices of X and Y . All distance entries are non-negative. Column 3: The top and bottom panels are the heat maps of $A = \{a_{ij}\}$ and $B = \{b_{ij}\}$, which are the properly centered distance matrices of \tilde{A} and \tilde{B} . The center panel is the heatmap of the entry-wise products of A and B , summing over which yields the un-normalized Mcorr statistic. As the entries of A and B can be either positive or negative, the entry-wise products can be either positive or negative for nonlinear dependencies, which causes $\text{Mcorr}(X, Y)$ to be close to 0 and the p-value to be in-significant, as shown in column 5. Column 4: The top and bottom panels are the heat maps of local A and B , i.e., $A^{k^*} = \{a_{ij}^{k^*}\}$ and $B^{l^*} = \{b_{ij}^{l^*}\}$, where $(k^*, l^*) = (4, 4)$ is the optimal scale for the circle relationship. The center panel is the heatmap of the entry-wise products of local A and B , summing over which yields the un-normalized Mgc statistic C^* . Mgc successfully identifies the optimal local structure for correlation testing, and the resulting entry-wise products are dominantly non-negative, which causes $\text{Mgc}(X, Y)$ to be much larger than 0 and the p-value to be significant, as shown in column 5. Column 5: The top panel is the testing powers of all local correlations, where the optimal scale is shown as a dark blue point with many adjacent scales being very close to optimal (light blue points). The bottom panel shows $\text{Mgc}(X, Y)$ and $\text{Mcorr}(X, Y)$ as dark and gray dots on the x-axis, as well as the distribution of the permuted test statistics.

165 $O(n^4)$ time. However, we have devised an algorithm for exactly computing *all* local correlations
166 in $\mathcal{O}(n^2 \log n)$, essentially the same running time complexity as global correlation coefficients (the
167 additional log factor is for sorting to find the neighbors, see Pseudocode 2 in Appendix D.1 for de-
168 tails). We do so by noting that the sufficient statistics for larger neighborhood sizes include those
169 for the smaller sizes, so we can simply keep track of them as we iteratively increase neighborhood
170 size. The end result is M_{GC} can be computed in time comparable to the other leading dependence
171 tests (see Pseudocode 3 in Appendix D.1 for details on computing all n^2 p-values efficiently).

172 Finally, we must find an optimal scale. Our procedure for estimating the optimal scale searches
173 for regions of neighborhood sizes for which p-values are consistently low, guarding against noisy
174 scales that appear optimal, and combating bias added by looking at many different scales. The
175 optimal scale is the largest neighborhood size in that region. The p-value of M_{GC} is therefore the
176 p-value of the optimal scale (see Pseudocode 4 and 5 in Appendix D.1 for details).

177 Finite Sample Simulation Experiments

178 We are interested in assessing the performance of our newly proposed multiscale tests in a wide
179 variety of settings, to better understand which the tests, and gain insight into which to use in
180 different settings. We therefore consider 20 different joint distributions f_{xy} corresponding to 20
181 different noisy dependence settings. A large fraction of these are taken exactly from existing
182 literature [9, 26–28], and we have added several additional settings. They include linear and nearly
183 linear (1-5), polynomial (6-12), trigonometric (13-17), uncorrelated but nonlinearly dependent (18-
184 19), and an independent relationship (20). Details for each setting are given in Appendix A, with
185 a visualization of each dependency shown in Supplementary Figure A1. For all 20 settings, we
186 define δ_x as Euclidean distance, $\delta(x_i, x_j) = \sum_{d=1}^{d_x} (x_i(d) - x_j(d))^2$, and the same for δ_y .

187 Figure 2 shows the testing powers versus the dimensionality of x (the dimensionality of y increases
188 in only a subset of the settings; see Methods for details), with the sample sizes fixed at $n = 100$ for
189 each setting. We compare our novel test, M_{GC} , with two previously proposed state-of-the-art tests:
190 $MCORR$ [10] and H_{HG} [28]. H_{HG} has previously been demonstrated to perform very well on all sorts
191 of nonlinear dependencies, especially in low-dimensional settings, and enjoys strong theoretical
192 guarantees. The advantage of M_{GC} over its global counterpart $MCORR$ and H_{HG} is stark. For the
193 nearly linear settings, M_{GC} and $MCORR$ are essentially identical and significantly better than H_{HG} as
194 the dimension increases. For the remaining nonlinear dependencies, M_{GC} achieves superior power

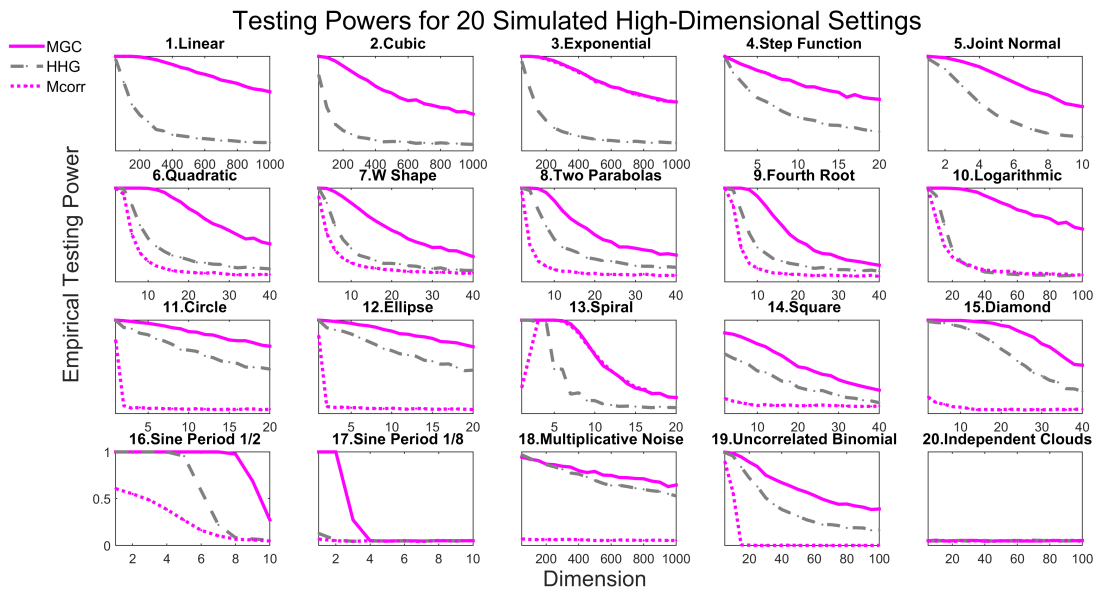


Figure 2: Powers of different methods for 20 different dependence structures, estimated by the empirical distributions of the test statistics under the null and the alternative on the basis of 10,000 Monte-Carlo replicates. 2,000 additional MC replicates are used for optimal scale estimation for Mgc. Each panel shows empirical testing power on the abscissa at a significant level $\alpha = 0.05$, and the dimensionality on the ordinate. Mgc empirically achieves similar or better power than the previous state of the art approaches for all sample sizes on all problems.

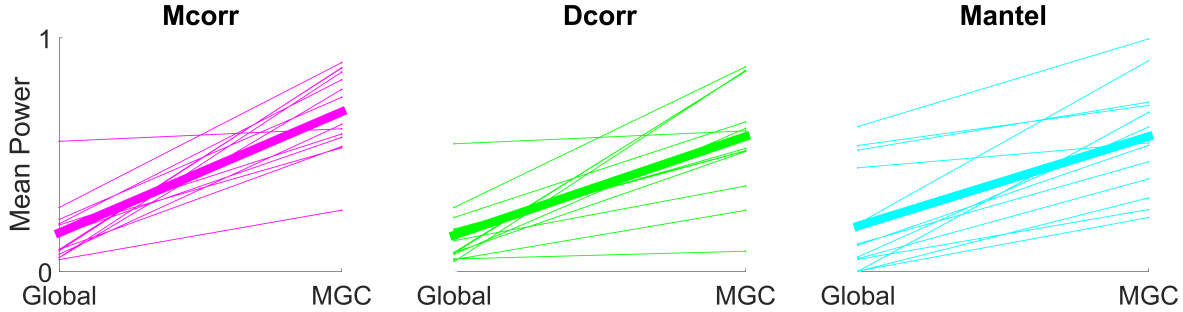


Figure 3: Average powers slopegraphs comparing global and MGC tests. For each global test, the left side corresponds to the mean power of each simulation in Figure 2, the right side corresponds to the respective MGC mean power. The thin solid lines are shown for 6-19, because MGC equals the global correlation for 1-5 and 20. Then the thick solid line summarizes how the overall mean power (including 6-19) changes from global to MGC. It is clear that MGC always significantly improves over its global counterpart.

195 than `HIG` and `MCORR` for *all* functions, often by a significant margin. For the independent simulation,
 196 all tests yield powers at the significance level α , indicating no more false positives than expected
 197 according to the theory. More exhaustive benchmark experiments, including focusing on the one-
 198 dimensional scenarios, in which we also compare to `MANTEL` and `Dcorr`, as well as our novel
 199 multiscale variants of both `MANTEL` and `Dcorr`, are qualitatively similar, and are therefore relegated
 200 to Appendix B.

201 MGC Empirically Dominates Global Counterparts

202 The above results demonstrate that converting `MCORR`, a global generalized correlation coefficient
 203 based test, to MGC, its multiscale variant, improves (or does not diminish) testing power for all
 204 considered settings, regardless of dimensionality. We wondered, therefore, whether the multiscale
 205 variant of other generalized correlation coefficients would behave similarly. Specifically we
 206 consider the `MANTEL` and `Dcorr` tests, in addition to `MCORR`, and for each, develop a multiscale
 207 variant (see Appendix C for details). Figure 3 show slopegraphs comparing global and multiscale
 208 generalized correlation coefficients. The top row shows for each of the 20 settings, with both x and
 209 y in 1-dimension, the average power as sample size increases. The bottom row shows the same,
 210 but keeping sample size fixed at $n = 100$ and increasing dimensionality of x . In all 40 settings, both
 211 low and increasing dimensions, and both fixed and increasing sample sizes, multiscale methods
 212 always improve on or stay the same, and never decrease power.

213 **Discovery of Dependency Across Scales**

214 A multiscale power map is a heatmap of powers for all neighborhood sizes, for a given joint distri-
215 bution and sample size. Figure 4 provides the multiscale power maps for all 20 different scenarios
216 for different dimensionalities, illustrating how the powers of local correlations change with respect
217 to increasing neighborhood sizes. The dimension was chosen as the largest one for which Mgc's
218 power exceeded 0.5, chosen to highlight the differences between scales.

219 The multiscale power map sheds light into the intrinsic dependency structure. For nearly linear
220 dependencies (1-5), the best neighborhood choice is always the largest scale, i.e., $k = l = n$.
221 For all strongly nonlinear dependencies (6-19), Mgc almost always chooses a smaller scale for x
222 or y . Furthermore, similar dependencies have similar local correlation structure, and thus similar
223 optimal scales. For example, quadratic (6) and W (7) are both polynomials of degree 2 with
224 different coefficients, and their power maps are quite similar to each other. Similarly, (16) and (17)
225 are the same trigonometry function (sine) with different periods, and they share a narrow range of
226 significant local correlations. Both circle (11) and eclipse (12), as well as square (14) and diamond
227 (15), are closely related functions, and have similar multiscale power maps. Note that for almost all
228 simulations, there exist a large portion of adjacent local neighborhoods that are equally significant,
229 which is an important observation that we use to approximate the optimal Mgc scale for real data.

230 **MGC Theoretically Dominates its Global Counterparts**

The formal testing scenario is as follows: we observe n pairs of observations, $(\mathbf{x}_i, \mathbf{y}_i)$, and we desire to know whether the \mathbf{x} 's are independent of the \mathbf{y} 's. To cast this problem as a statistical inference query requires specifying a statistical model, that is, a collection of possible distributions from which we may assume the data arise. To make the investigation as general as possible, we consider the largest possible set of distributions: any possible joint distribution f_{xy} . If \mathbf{x} and \mathbf{y} were independent, then it would follow that $f_{xy} = f_x f_y$; in other words, for independent data, the joint distribution is equal to the product of the marginals. Therefore, we have the following hypothesis testing scenario:

$$H_0 : f_{xy} = f_x f_y,$$

$$H_A : f_{xy} \neq f_x f_y.$$

231 The power of a test is defined as the probability that it correctly rejects the null when the null is

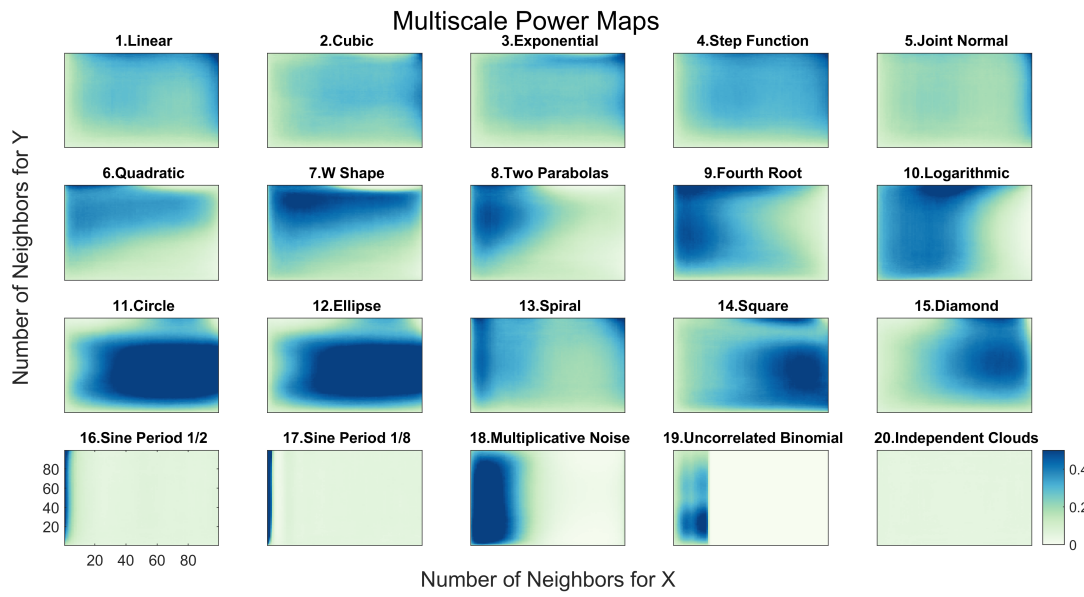


Figure 4: Influence of neighborhood size on testing power of local correlations at $\alpha = 0.05$. For each of the 20 panels, the abscissa denotes the number of neighbors for X (the scale increases from left to right), and the ordinate denotes the number of neighbors for Y (the scale increases from bottom to top). For each simulation, the sample size is $n = 100$, and the dimension is determined by the largest dimension for Mgc to have powers exceeding the threshold 0.5. Each different simulation yields a different surface, highlighting the importance of understanding local scale in terms of understanding the data.

indeed false. As defined above, a test is consistent if its power converges to 1 as sample size increases. Let C_t denote a global generalized correlation coefficient based test, that is, t might indicate MANTEL, Dcorr, or Mcorr, and let $\beta(C_t^*)$ denote the power of the corresponding multiscale version. Recall from the work Szekeley et al. that Dcorr and Mcorr are both consistent tests. More specifically, Dcorr is consistent whenever f_{xy} has finite dimension and bounded variance, and Mcorr is consistent even as dimension increases to infinity. Denote the set of distributions satisfying consistency for a given test by \mathcal{F}_t , where t indicates which test we are referring to. Then, we have the following theorem:

Theorem 1. $\beta(C_t^*) \rightarrow 1$ for all f_{xy} in \mathcal{F}_t .

Therefore, Mgc is consistent against all dependent alternatives for which its global counterpart is. For finite samples, however, things appear more interesting. For linear dependencies, the optimal Mgc scale was empirically always the global one. We therefore conjectured and proved the following:

Theorem 2. If x is linearly dependent on y , then for any n it always holds that

$$\beta(C^{nn}) = \beta(C^*) = \beta(C). \quad (4)$$

Thus the optimal scale for Mgc is the global scale for linearly dependent data.

Second, under certain nonlinear dependencies, Mgc can achieve a better finite-sample testing power than its corresponding global correlation. Indeed, we were able to prove both of these claims:

On the other hand, for finite sample nonlinear dependencies (which better characterize all real data), we note that Mgc almost always improves upon its global counterpart. We therefore conjectured and proved the following:

Theorem 3. There exists f_{xy} and n such that

$$\beta(C^*) > \beta(C). \quad (5)$$

Thus multiscale graph correlation can be better than its global correlation coefficient under certain nonlinear dependency, for finite sample.

256 Note that Theorem 2 and Theorem 3 hold for any of M_GC varieties, including D_{CORR}, M_{CORR}, and
257 M_{ANTEL}. The proofs of Theorem 2 and 3 are both in Appendix E. The proof of Theorem 2 is
258 straightforward. The proof of Theorem 3 is a constructive one. More specifically, we constructed
259 quadratic function and sampled data a finite number of times and exactly compute the power for
260 both M_GC and D_{CORR}, proving that M_GC has higher power in this setting. This shows that M_GC can
261 outperform its global counterpart even for the most modest nonlinear functions. Because any
262 function can be approximated by a polynomial expansion [29], the proof of Theorem 3 suggests
263 that M_GC is able to outperform its corresponding global correlation on a wide variety of nonlinear
264 functions, which is indeed the case throughout the numerical simulations. To our knowledge,
265 Theorems 2 and 3 are the first finite sample theorems for dependence testing.

266 The three above theorems taken together lead to the main theoretical result of this manuscript:

267 **Theorem 4.** *M_GC dominates its global counterpart, meaning that M_GC is always as good as, and
268 sometimes better than, its corresponding global correlation coefficient.*

269 Real Data Experiments

270 Only Local Scales can Detect Dependence

271 Our first real data experiment investigates whether brain shape and disease status are dependent
272 on one another. Previous investigations have linked major depressive disorder to the hippocampus
273 shape [3, 30], though global tests were unable to detect a statistically significant dependence
274 structure at the $\alpha = 0.05$ level.

275 This brain shape versus disease dataset consists of $n = 114$ subjects, for each we have an
276 MRI scan as well as a categorical variable indicating whether the subject is clinically depressed,
277 high-risk, or non-affected. From the MRI data, previous work extracted both the left and right
278 hippocampi. For the brain shape “view” of the data, they computed the interpoint comparison
279 matrices using a nonlinear landmark matching approach [3, 31]. For the categorical disorder
280 variable, we use squared Euclidean distance, then add 1 to every non-diagonal entry (so only the
281 diagonals are of distance 0).

282 We consider two dependence tests, one for each hemisphere: is hippocampus shape indepen-
283 dent of depressive state. Figure 5A provides the p-value curves for M_GC for $k = 2, \dots, n$ at $l = 4$
284 (we only show $l = 4$ because the other curves look similar). Many local scales yield significant p-

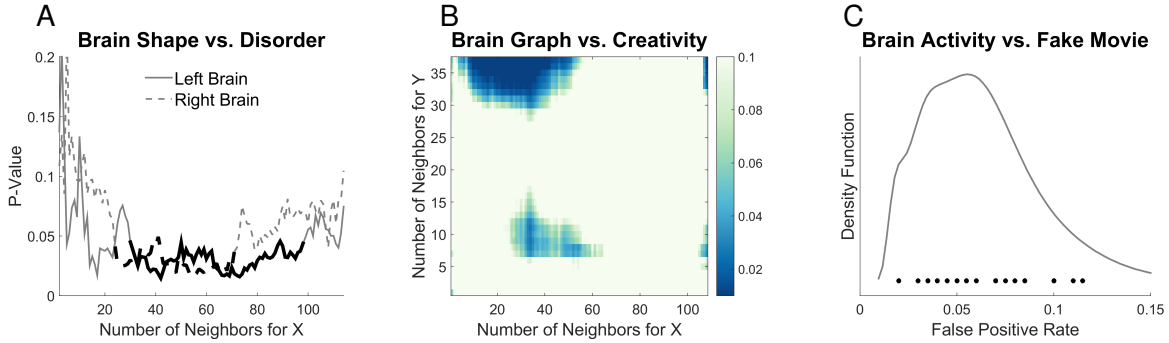


Figure 5: (A) Local correlation p-value curves with respect to $k = 2, \dots, 114$ at $l = 4$ for brain vs disease. Dark lines correspond to the largest region of significant scales. (B) Local correlation p-value heat map with respect to $k = 2, \dots, 109$ and $l = 2, \dots, 38$ for brain MIGRAINE vs CCI. (C) Density estimate for the false positive rates of MGC on the brain vs noise experiments, with the actual rate of each data shown as dots above the x-axis.

values (around 0.01) for both hemispheres, whereas the global scale does not detect a significant dependence in either hemisphere. None of the previously proposed dependence tests under consideration (MANTEL, DCORR, MCORR, or HHG) were able to detect dependence for both hemispheres (not shown).

289 MGC can provide insight into the nature of the dependence structure

The next real data experiment investigates whether brain networks and personalities are independent of one another. Previous work [32] investigated whether individual voxels were related to specific dimensions of personality, but were unable to compare entire brain networks to a higher-dimensional characterization of personality. In this dataset, we have $n = XXX$ subjects, for each we obtained a resting-state functional MRI scan as well as her five-factor personality trait as quantified by the NEO Personality Inventory-Revised [33].

Figure 5B shows that global dependence tests can ascertain whether the whole brain-network is independent of the subject's personality. However, the global test is quite fragile, even ignoring a single subject from the global test can render the test non-significant. On the other hand, MGC is more robust, there is a whole region of neighborhood sizes such that the test is quite significant. Moreover, that the local tests performs optimally with approximately 30 neighbors suggests that these data have multiple cohorts, for which the dependence structure likely differs. This result therefore suggests the next investigatory steps to take to further understand the nature of the

303 dependence structure between brain networks and personality.

304 **MGC Does Not Inflate False Positive Rates**

305 In the last experiment, MGC is applied to test independence between brain voxel activities and non-
306 existent stimulus similar to a pair of studies led by Eklund et al. [34, 35], by using 26 resting state
307 fMRI data sets from the 1000 functional connectomes project ([http://fcon_1000.projects.
308 nitrc.org/](http://fcon_1000.projects.nitrc.org/)), consisting of a total of XXX subjects. We used CPAC [36] to estimate regional
309 time-series, in particular, using the sequence of pre-processing decisions determined to optimize
310 discriminability [37]. The output for each scan is the resting state fMRI time-series data containing
311 200 regions of interest for 200 time-steps. We then also generate an independent stimulus by sam-
312 pling from a standard normal at each time step. Of course, the brain activity data and the stimuli
313 are independent by construction. For each brain region, we test: is activity of that brain region
314 independent of the time-varying stimuli. We pool brain activity over all of the samples from the
315 population. Any regions that are detected significant are false positives by definition. By testing
316 each brain region separately, we obtain a distribution of false positive rates. If our test is unbi-
317 ased, that distribution should be centered around the critical level, which we set at 0.05 for this
318 experiment.

319 To conduct this test, we must construct a distance matrix for brain region activity, and another for
320 the stimulus. For each brain region, we compute $a_{ij} = \|\mathbf{x}_{\cdot i} - \mathbf{x}_{\cdot j}\|_2^2$, for all (i, j) pairs, where $\mathbf{x}_{\cdot i}$
321 denotes the observation vector of all subjects at time-step i . For the stimulus, we similarly compute
322 the Euclidean distance between activity at all pairs of time-steps: $b_{ij} = (y_i - y_j)^2$. Note that the
323 distance matrices at different brain regions are distinct, but the stimulus is the same for all brain
324 regions during the same experiment.

325 For each data set, the above test is carried out for each brain region, and the false positive rates of
326 MGC for each dataset are shown in Figure 5C. MGC false positive rate is centered around the critical
327 level 0.05, as it should be. In contrast, standard methods for fMRI analysis, such as generalized
328 linear models, significantly increase or decrease the false discovery rates, depending on the data
329 [34, 35].

330 **Discussion**

331 We propose multiscale graph correlation to test independence between measurement types. We
332 demonstrate via simulations that MGC empirically performs well in linear and non-linear settings,
333 regardless of the dimension, sample size, and noise statistics. Moreover, it efficiently adapts
334 to the data, to provide not just a valid p-value, but also a picture of which scales contain the
335 dependence structure. We then prove that it dominates global generalized correlation coefficients
336 in finite samples, the first finite sample theorems for dependence testing that we are aware of. In
337 real data experiments MGC reveals dependence where global methods fail, discovers the scale of
338 dependence where global methods succeeded, and did not falsely detect signals when there were
339 none.

340 A method closely related to distance correlation tests arises from the machine learning commu-
341 nity: kernel-based independence test [38–40]. Recent work has demonstrated the equivalence
342 between these kernel tests and the energy statistics work [41, 42]. Thus, we may be able to glean
343 further insights by casting MGC within the kernel framework. Specifically, more efficient tests using
344 asymptotic null distribution approximations are possibly available.

345 Two other tests merit particular mention at this point. First, Dumcke et al [43] recently proposed a
346 related nearest-neighbor based test. Unfortunately, their proposed test requires estimating relative
347 high-dimensional densities, and therefore, does not perform particularly well, nor does it have
348 strong theoretical support. Finally, Reshef et al [44] is another dependence testing methodology,
349 but does not perform as well as energy based tests in various benchmarks [26], and is designed
350 specifically for low-dimensional settings.

351 While in this work we proved that there exist scales that improve upon the global scale, we did not
352 yet prove that the scale we do select is optimal. Figure A2 shows that our estimated scales are
353 accurate

354 Furthermore, the optimal scale for MGC is also of interest, such as how to more accurately select the
355 local scale under unknown models for a particular inference task, and the implication of the optimal
356 scale on the geometry of underlying dependency, etc. Another direction we are investigating is
357 how to choose the optimal metric for given data. Beyond the dependence testing framework, it may
358 also be promising to pursue the applications of MGC and local correlations in other closely-related
359 subjects, such as dimension reduction, classification, other testing and prediction domains, etc.

360 **References**

- 361 [1] K. Pearson, *Proceedings of the Royal Society of London* **58**, 240 (1895). 3, 4
- 362 [2] M. Reimherr, D. Nicolae, *Statistical Science* **28**, 116 (2013). 3
- 363 [3] Y. Park, C. Priebe, M. Miller, N. Mohan, K. Botteron, *Journal of Biomedicine and Biotechnol-*
364 *ogy* p. 694297 (2008). 3, 14
- 365 [4] J. Maa, D. Pearl, R. Bartoszynski, *Annals of Statistics* **24**, 1069 (1996). 3, 4
- 366 [5] W. K. Allard, G. Chen, M. Maggioni, *Applied and Computational Harmonic Analysis* **32**, 435
367 (2012). 3, 4
- 368 [6] M. G. Kendall, *Rank Correlation Methods* (London: Griffin, 1970). 4
- 369 [7] C. Spearman, *The American Journal of Psychology* **15**, 72 (1904). 4
- 370 [8] N. Mantel, *Cancer Research* **27**, 209 (1967). 4, 27
- 371 [9] G. Szekely, M. Rizzo, N. Bakirov, *Annals of Statistics* **35**, 2769 (2007). 4, 8, 20, 28, 39
- 372 [10] G. Szekely, M. Rizzo, *Journal of Multivariate Analysis* **117**, 193 (2013). 4, 8, 29, 39
- 373 [11] R. Lyons, *Annals of Probability* **41**, 3284 (2013). 4, 28
- 374 [12] C. Stone, *Annals of Statistics* **4**, 595 (1977). 4
- 375 [13] I. Daubechies, *Ten lectures on wavelets* (SIAM, 1992). 5
- 376 [14] B. Sarwar, G. Karypis, J. Konstan, J. Riedl, *ACM WebKDD 2000 Workshop* (2000). 5
- 377 [15] W. Torgerson, *Multidimensional Scaling: I. Theory and method* (Psychometrika, 1952). 5
- 378 [16] J. B. Tenenbaum, V. de Silva, J. C. Langford, *Science* **290**, 2319 (2000). 5
- 379 [17] V. de Silva, J. B. Tenenbaum, *Advances in Neural Information Processing Systems* **15**, 721
380 (2003). 5
- 381 [18] L. K. Saul, S. T. Roweis, *Science* **290**, 2323 (2000). 5
- 382 [19] S. T. Roweis, L. K. Saul, *Journal of Machine Learning Research* **4**, 119 (2003). 5
- 383 [20] M. Belkin, P. Niyogi, *Neural Computation* **15**, 1373 (2003). 5

- 384 [21] D. Barton, F. David, *Research Papers in Statistics*, Wiley, New York (1966). 5
- 385 [22] J. Friedman, L. Rafsky, *Annals of Statistics* **11**, 377 (1983).
- 386 [23] M. Schilling, *Journal of the American Statistical Association* **81**, 799 (1986). 5
- 387 [24] C. Shen, J. T. Vogelstein, C. Priebe, *Submitted* (2016). 5
- 388 [25] P. Good, *Permutation, Parametric, and Bootstrap Tests of Hypotheses* (Springer, 2005). 6
- 389 [26] N. Simon, R. Tibshirani, available at <http://arxiv.org/abs/1401.7645> (2012). 8, 17, 20
- 390 [27] M. Gorfine, R. Heller, Y. Heller, available at <http://ie.technion.ac.il/~gorfinm/files/science6.pdf> (2012). 20, 31
- 392 [28] R. Heller, Y. Heller, M. Gorfine, *Biometrika* **100**, 503 (2013). 8, 31
- 393 [29] W. Rudin, *Real and Complex Analysis* (McGraw-Hill Education, 1986), third edn. 14
- 394 [30] J. Posener, et al., *American Journal of Psychiatry* **160**, 83 (2003). 14
- 395 [31] M. Beg, M. Miller, A. Trouv, L. Younes, *International journal of computer vision* **61**, 139 (2005).
396 14
- 397 [32] J. Adelstein, et al., *PLoS ONE* **6**, e27633 (2011). 15
- 398 [33] R. R. Costa, & McCrae, *Neo PI-R professional manual*, vol. 396 (1992). 15
- 399 [34] A. Eklund, M. Andersson, C. Josephson, M. Johannesson, H. Knutsson, *NeuroImage* **61**, 565
400 (2012). 16
- 401 [35] A. Eklund, T. Nichols, H. Knutsson, *arXiv* (2015). 16
- 402 [36] C. Craddock, et al., *Frontiers in Neuroinformatics* **42** (2015). 16
- 403 [37] S. Wang, C. E. Priebe, M. Maggioni, J. T. Vogelstein, *in preparation* (2016). 16
- 404 [38] A. Gretton, R. Herbrich, A. Smola, O. Bousquet, B. Scholkopf, *Journal of Machine Learning
405 Research* **6**, 2075 (2005). 17
- 406 [39] A. Gretton, L. Gyorfi, *Journal of Machine Learning Research* **11**, 1391 (2010).
- 407 [40] A. Gretton, K. Borgwardt, M. Rasch, B. Scholkopf, A. Smola, *Journal of Machine Learning
408 Research* **13**, 723 (2012). 17

- 409 [41] D. Sejdinovic, B. Sriperumbudur, A. Gretton, K. Fukumizu, *Annals of Statistics* **41**, 2263
 410 (2013). [17](#)
- 411 [42] A. Ramdas, S. J. Reddi, B. Pcos, A. Singh, L. Wasserman, *29th AAAI Conference on Artifi-*
 412 *cial Intelligence* (2015). [17](#)
- 413 [43] S. Dmcke, U. Mansmann, A. Tresch, *PLOS ONE* **9**, e107955 (2014). [17](#)
- 414 [44] D. Reshef, *et al.*, *Science* **334**, 1518 (2011). [17](#)

415 Acknowledgment

416 This work was partially supported by National Security Science and Engineering Faculty Fellow-
 417 ship (NSSEFF), Johns Hopkins University Human Language Technology Center of Excellence
 418 (JHU HLT COE), Defense Advanced Research Projects Agency's (DARPA) SIMPLEX program
 419 through SPAWAR contract N66001-15-C-4041, and the XDATA program of the Defense Advanced
 420 Research Projects Agency (DARPA) administered through Air Force Research Laboratory con-
 421 tract FA8750-12-2-0303. The authors thank Dr. Brett Mensh of Optimize Science for acting as our
 422 intellectual consigliere.

423 A Simulation Functions

424 We list the distributions of the 20 dependencies used in the simulations, which are based on a
 425 combination of the simulations used in [9, 26, 26, 27] but with some changes (such as the inclusion
 426 of additional noise and an extra weight vector) to better compare all methods throughout different
 427 dimensions and sample sizes.

428 For each sample $x \in \mathbb{R}^{d_x}$, we denote $x^d, d = 1, \dots, d_x$ as the d th dimension of x . For the purpose
 429 of high-dimensional simulations, $w \in \mathbb{R}^{d_x}$ is a decaying vector with $w^d = 1/d$ for each d , such
 430 that $w^T x$ is a 1-dimensional weighted summation of all dimensions of x , which equals x if $d_x = 1$.
 431 Furthermore, \mathcal{U} denotes the uniform distribution, \mathcal{B} denotes the Bernoulli distribution, \mathcal{N} denotes
 432 the normal distribution, u and v represent realizations from some auxiliary random variables, c is
 433 a scalar constant to control the noise level (which equals 1 for 1-dimensional simulations and 0

⁴³⁴ otherwise), and ϵ is sampled from an independent standard normal distribution unless mentioned
⁴³⁵ otherwise.

⁴³⁶ For all of the below equations, $(\mathbf{x}, \mathbf{y}) \stackrel{iid}{\sim} f_{xy} = f_{y|x}f_x$. For each setting, we provide the space of
⁴³⁷ (\mathbf{x}, \mathbf{y}) , and define each of the above distributions, and any additional auxiliary distributions.

1. Linear $(\mathbf{x}, \mathbf{y}) \in \mathbb{R}^{d_x} \times \mathbb{R}$,

$$\mathbf{x} \sim \mathcal{U}(-1, 1)^{d_x},$$

$$\mathbf{y} = w^\top \mathbf{x} + c\epsilon.$$

2. Cubic $(\mathbf{x}, \mathbf{y}) \in \mathbb{R}^{d_x} \times \mathbb{R}$:

$$\mathbf{x} \sim \mathcal{U}(-1, 1)^{d_x},$$

$$\mathbf{y} = 128(w^\top \mathbf{x} - \frac{1}{3})^3 + 48(w^\top \mathbf{x} - \frac{1}{3})^2 - 12(w^\top \mathbf{x} - \frac{1}{3}) + 80c\epsilon.$$

3. Exponential $(\mathbf{x}, \mathbf{y}) \in \mathbb{R}^{d_x} \times \mathbb{R}$:

$$\mathbf{x} \sim \mathcal{U}(0, 3)^{d_x},$$

$$\mathbf{y} = \exp(w^\top \mathbf{x}) + 10c\epsilon.$$

4. Step Function $(\mathbf{x}, \mathbf{y}) \in \mathbb{R}^{d_x} \times \mathbb{R}$:

$$\mathbf{x} \sim \mathcal{U}(-1, 1)^{d_x},$$

$$\mathbf{y} = I(w^\top \mathbf{x} > 0) + \epsilon,$$

⁴³⁸ where I is the indicator function.

5. Joint normal $(\mathbf{x}, \mathbf{y}) \in \mathbb{R}^{d_x} \times \mathbb{R}^{d_x}$: Let $\rho = 1/2d_x$, I_{d_x} be the identity matrix of size $d_x \times d_x$,
 J_{d_x} be the matrix of ones of size $d_x \times d_x$, and $\Sigma = \begin{bmatrix} I_{d_x} & \rho J_{d_x} \\ \rho J_{d_x} & I_{d_x} \end{bmatrix}$. Then let $(u, v) \sim \mathcal{N}(0, \Sigma)$,
 $\epsilon \sim \mathcal{N}(0, I_{d_x})$,

$$\mathbf{x} = u,$$

$$\mathbf{y} = v + 0.5c\epsilon.$$

6. Quadratic $(\mathbf{x}, \mathbf{y}) \in \mathbb{R}^{d_x} \times \mathbb{R}$:

$$\mathbf{x} \sim \mathcal{U}(-1, 1)^{d_x},$$

$$\mathbf{y} = (w^\top \mathbf{x})^2 + 0.5c\epsilon.$$

7. W Shape $(\mathbf{x}, \mathbf{y}) \in \mathbb{R}^{d_x} \times \mathbb{R}$: $u \sim \mathcal{U}(-1, 1)^{d_x}$,

$$\begin{aligned}\mathbf{x} &\sim \mathcal{U}(-1, 1)^{d_x}, \\ \mathbf{y} &= 4 \left[\left((w^\top \mathbf{x})^2 - \frac{1}{2} \right)^2 + w^\top u / 500 \right] + 0.5c\epsilon.\end{aligned}$$

8. Two Parabolas $(\mathbf{x}, \mathbf{y}) \in \mathbb{R}^{d_x} \times \mathbb{R}$: $\epsilon \sim \mathcal{U}(0, 1)$, $u \sim \mathcal{B}(0.5)$,

$$\begin{aligned}\mathbf{x} &\sim \mathcal{U}(-1, 1)^{d_x}, \\ \mathbf{y} &= ((w^\top \mathbf{x})^2 + 2c\epsilon) \cdot (u - \frac{1}{2}).\end{aligned}$$

9. Fourth Root $(\mathbf{x}, \mathbf{y}) \in \mathbb{R}^{d_x} \times \mathbb{R}$:

$$\begin{aligned}\mathbf{x} &\sim \mathcal{U}(-1, 1)^{d_x}, \\ \mathbf{y} &= |w^\top \mathbf{x}|^{\frac{1}{4}} + \frac{c}{4}\epsilon.\end{aligned}$$

10. Logarithmic $(\mathbf{x}, \mathbf{y}) \in \mathbb{R}^{d_x} \times \mathbb{R}^{d_x}$: $\epsilon \sim \mathcal{N}(0, I_{d_x})$

$$\begin{aligned}\mathbf{x} &\sim \mathcal{N}(0, I_{d_x}), \\ \mathbf{y}^d &= 2\log(\mathbf{x}^d) + 3c\epsilon^d,\end{aligned}$$

439 **for** $d = 1, \dots, d_x$.

11. Circle $(\mathbf{x}, \mathbf{y}) \in \mathbb{R}^{d_x} \times \mathbb{R}$: $u \sim \mathcal{U}(-1, 1)^{d_x}$, $\epsilon \sim \mathcal{N}(0, I_{d_x})$, $r = 1$,

$$\begin{aligned}\mathbf{x}^d &= r \left(\sin(\pi u^{d+1}) \prod_{j=1}^d \cos(\pi u^j) + 0.4\epsilon^d \right) \text{ for } d = 1, \dots, d_x - 1, \\ \mathbf{x}^{d_x} &= r \left(\prod_{j=1}^{d_x} \cos(\pi u^j) + 0.4\epsilon^{d_x} \right), \\ \mathbf{y} &= \sin(\pi u^1).\end{aligned}$$

440 12. Ellipse $(\mathbf{x}, \mathbf{y}) \in \mathbb{R}^{d_x} \times \mathbb{R}$: Same as above except $r = 5$.

13. Spiral $(\mathbf{x}, \mathbf{y}) \in \mathbb{R}^{d_x} \times \mathbb{R}$: $u \sim \mathcal{U}(0, 5)$, $\epsilon \sim \mathcal{N}(0, 1)$,

$$\begin{aligned}\mathbf{x}^d &= u \sin(\pi u) [\cos(\pi u)]^d \text{ for } d = 1, \dots, d_x - 1, \\ \mathbf{x}^{d_x} &= u [\cos(\pi u)]^{d_x}, \\ \mathbf{y} &= u \sin(\pi u) + 0.4(d_x - 1)\epsilon.\end{aligned}$$

14. Square $(\mathbf{x}, \mathbf{y}) \in \mathbb{R}^{d_x} \times \mathbb{R}^{d_x}$: Let $u \sim \mathcal{U}(-1, 1)$, $v \sim \mathcal{U}(-1, 1)$, $\epsilon \sim \mathcal{N}(0, 1)^{d_x}$, $\theta = -\frac{\pi}{8}$. Then

$$\begin{aligned}\mathbf{x}^d &= u \cos \theta + v \sin \theta + 0.05d_x \epsilon^d, \\ \mathbf{y}^d &= -u \sin \theta + v \cos \theta,\end{aligned}$$

441 **for** $d = 1, \dots, d_x$.

442 15. Diamond $(\mathbf{x}, \mathbf{y}) \in \mathbb{R}^{d_x} \times \mathbb{R}^{d_x}$: Same as above except $\theta = -\frac{\pi}{4}$.

16. Sine Period 1/2 $(\mathbf{x}, \mathbf{y}) \in \mathbb{R}^{d_x} \times \mathbb{R}$: $u \sim \mathcal{U}(-1, 1)$, $v \sim \mathcal{N}(0, 1)^{d_x}$, $\theta = 4\pi$,

$$\mathbf{x}^d = u + 0.02d_x v^d \text{ for } d = 1, \dots, d_x,$$

$$\mathbf{y} = \sin(\theta x) + c\epsilon.$$

443 17. Sine Period 1/8 $(\mathbf{x}, \mathbf{y}) \in \mathbb{R}^{d_x} \times \mathbb{R}$: Same as above except $\theta = 16\pi$ and the noise is changed
444 to $0.5c\epsilon$.

18. Multiplicative Noise $(\mathbf{x}, \mathbf{y}) \in \mathbb{R}^{d_x} \times \mathbb{R}^{d_x}$: $u \sim \mathcal{N}(0, I_{d_x})$, $\epsilon \sim \mathcal{N}(0, I_{d_x})$,

$$\mathbf{x} \sim \mathcal{N}(0, I_{d_x}),$$

$$\mathbf{y}^d = u^d \mathbf{x}^d + 0.5\epsilon^d,$$

445 for $d = 1, \dots, d_x$.

19. Uncorrelated Binomial $(\mathbf{x}, \mathbf{y}) \in \mathbb{R}^{d_x} \times \mathbb{R}$: $u \sim \mathcal{B}(0.5)$,

$$\mathbf{x} \sim \mathcal{B}(0.5)^{d_x},$$

$$\mathbf{y} = (2u - 1)w^\top \mathbf{x} + 0.6\epsilon.$$

20. Independent Clouds $(\mathbf{x}, \mathbf{y}) \in \mathbb{R}^{d_x} \times \mathbb{R}^{d_x}$: Let $u \sim \mathcal{N}(0, I_{d_x})$, $v \sim \mathcal{N}(0, I_{d_x})$, $u' \sim \mathcal{B}(0.5)^{d_x}$,
 $v' \sim \mathcal{B}(0.5)^{d_x}$. Then

$$\mathbf{x} = u/3 + 2u' - 1,$$

$$\mathbf{y} = v/3 + 2v' - 1.$$

446 For each distribution, \mathbf{x} and \mathbf{y} are clearly dependent except (20); for some settings (11-15) they
447 are conditionally independent upon conditioning on the respective auxiliary variables, while for
448 others they are "directly" dependent. Then we can independently generate (x_i, y_i) from (\mathbf{x}, \mathbf{y}) for
449 $i = 1, \dots, n$, set $X = [x_1, \dots, x_n] \in \mathbb{R}^{d_x \times n}$ and $Y = [y_1, \dots, y_n] \in \mathbb{R}^{d_y \times n}$, and calculate local /
450 global correlations for the sample data. A visualization of each dependency is shown in Figure A1.

451 For the increasing dimension simulation in the main paper, we always set $c = 0$ and $n = 100$,
452 with d_x increasing while $d_y = d_x$ for type 5, 10, 14, 15, 18, 20 and $d_y = 1$ otherwise. The decaying
453 vector w is utilized for $d_x > 1$ to treat higher dimensions as small perturbations, which creates a
454 meaningful setting for testing power comparison. The powers of all three Mgc implementations in
455 this setting are provided in Figure A3, where we denote Mgc_D as the Mgc for Dcorr, Mgc_M as the
456 Mgc for Mcorr, Mgc_P as the Mgc for Mantel.

B Supplementary Results

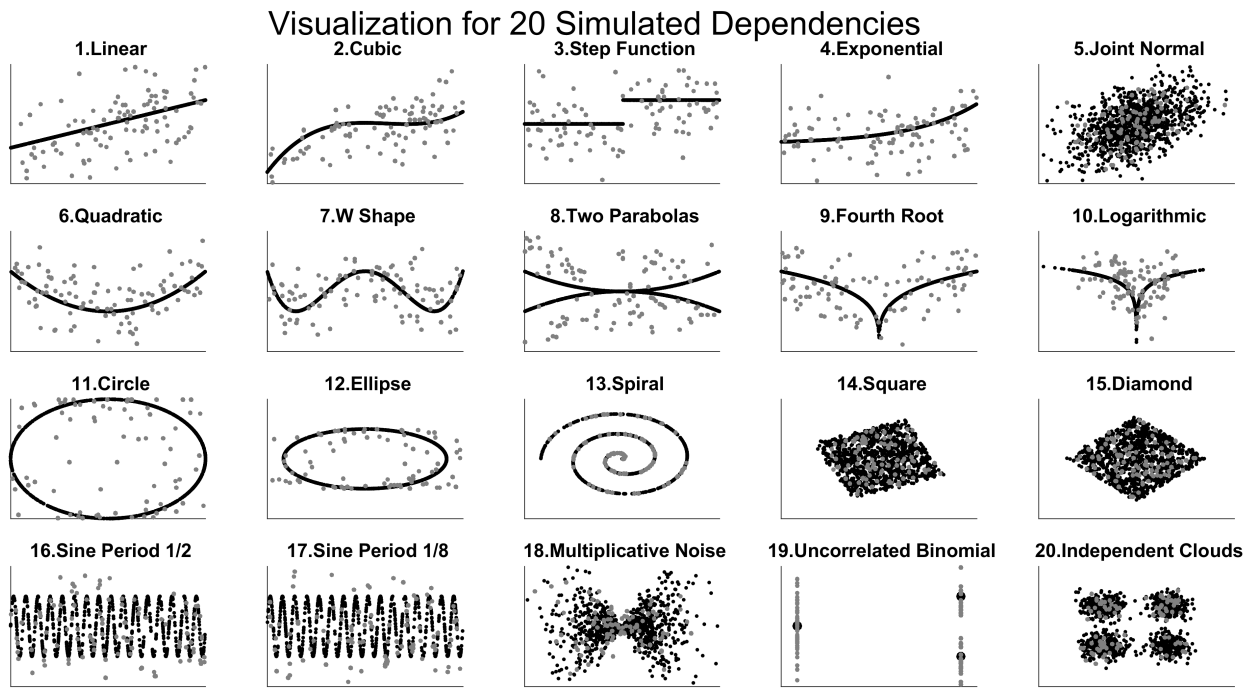


Figure A1: Visualization of the 20 dependencies for 1-dimensional simulations. The blue points are generated with noise ($c=1$) at $n = 100$ to show the actual sample data in testing, and the red points are generated without noise at $n = 1000$ to highlight each underlying dependency.

458 Here we also present an additional setting, which sets $d_x = d_y = 1$ and $c = 1$ with the sample size
 459 n increasing from 5 to 100. The parameter before c (e.g., there is a 80 before c in type 2) is a tuned
 460 noise parameter for some dependencies, so the testing powers can be compared meaningfully
 461 for each simulation, i.e., in the absence of noise, the testing powers may converge to 1 at very
 462 small n for some trivial dependencies like linear; and it is also more meaningful to consider noisy
 463 simulations in practice. The powers of all methods in this setting are provided in Figure A4, with
 464 the multiscale power maps shown in Figure A5.

465 Clearly MGC always improves over its global counterpart, and always has a large advantage re-
 466 gardless of the underlying dependency structure, the dimensionality, the sample size, or noise.

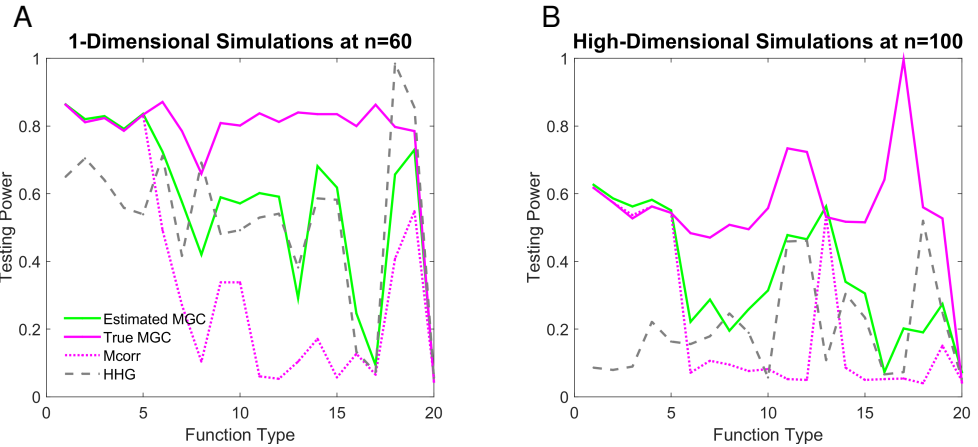


Figure A2: Comparing estimated Mgc power to true Mgc power, for the 1-dimensional and high-dimensional simulations. (A) 1-dimensional simulations, where $d_x = 1$ and the sample size is chosen by the power threshold 0.8 as in Figure A5. (B) High-dimensional simulations, where $n = 100$ and the dimension is chosen by the power threshold 0.5 as in Figure 4. The estimated Mgc power by the approximated optimal scale is almost always better than global MCORR and HHG, combines the better performance of the two benchmarks, is quite close to the true Mgc power, and does not inflate false signals.

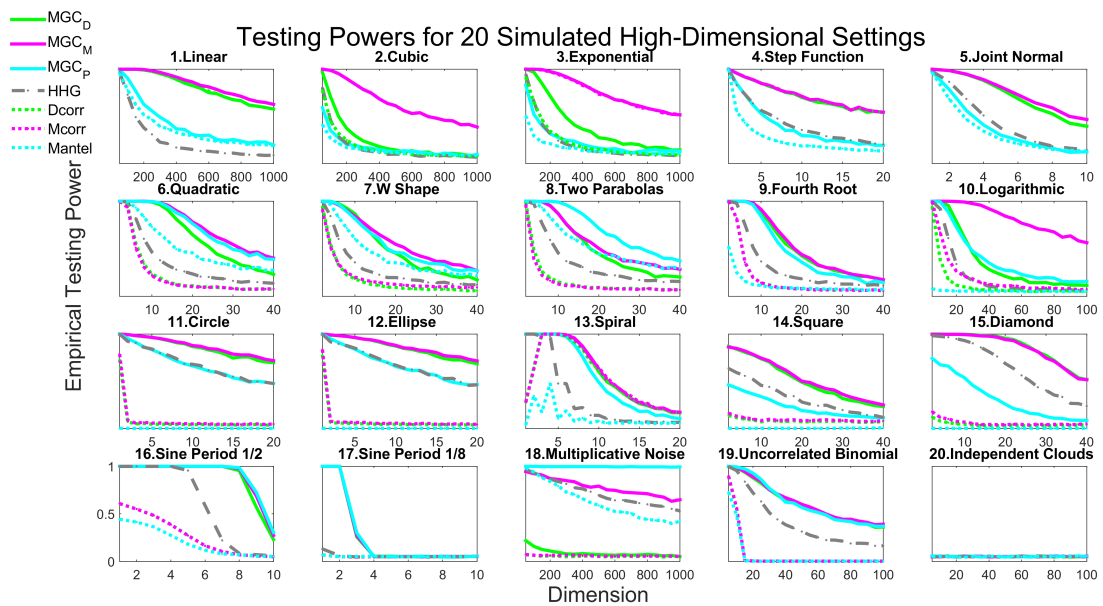


Figure A3: Same as Figure 2 but includes all three different Mgc implementations.

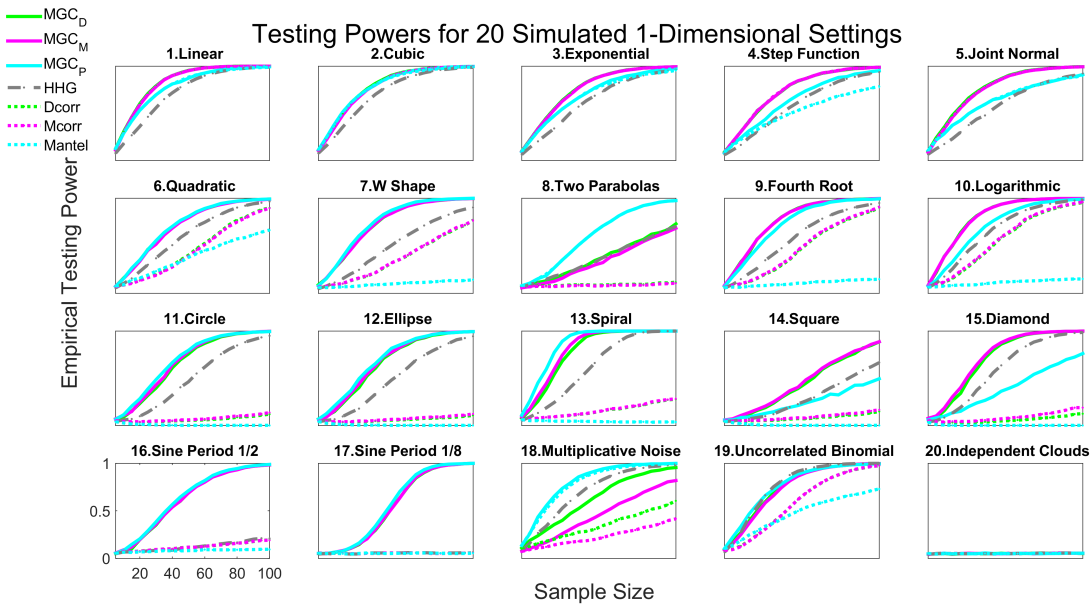


Figure A4: Powers of different methods for 20 different 1-dimensional dependence structures, estimated by the empirical distributions of the test statistics under the null and the alternative on the basis of 10,000 Monte-Carlo replicates. 2,000 additional MC replicates are used for optimal scale estimation for Mgc . Each panel shows empirical testing power on the abscissa at a significant level $\alpha = 0.05$, and sample size on the ordinate. Mgc empirically achieves similar or better power than the previous state of the art approaches for all sample sizes on nearly all problems.

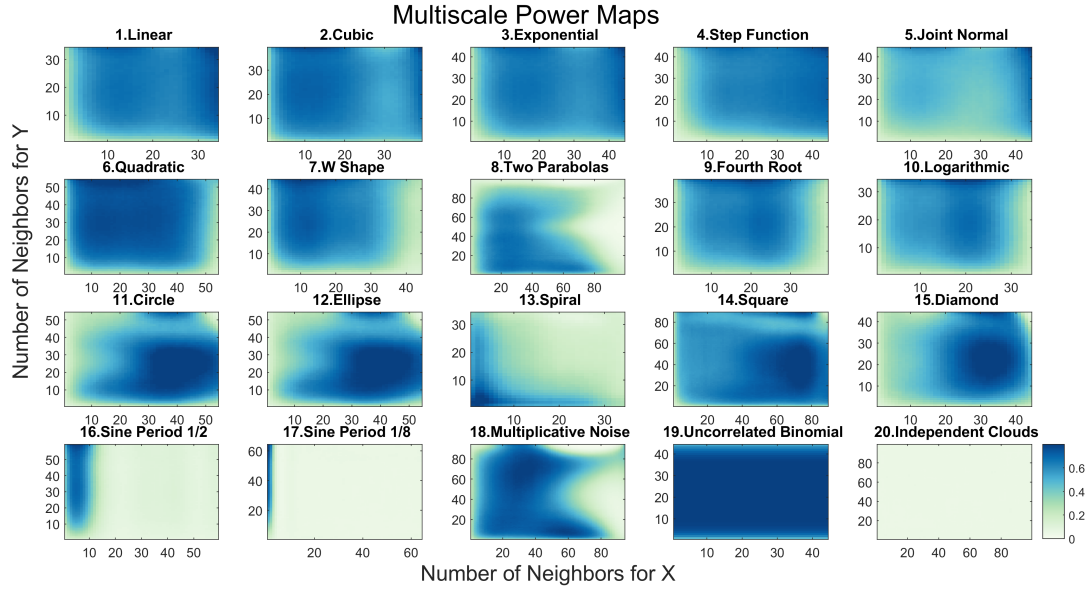


Figure A5: Influence of neighborhood size on testing power of local correlations. For each simulation, the dimension is 1, and the sample size is determined by the first sample size n for MGC to have powers exceeding the threshold 0.8.

467 C Dependence Measures

468 In this section, we review the MANTEL test, distance correlation, modified distance correlation, the
 469 MGC statistic, and the H_{HG} statistic in order. Note that for DCORR / MCORR, we implement them in a
 470 slightly different but equivalent way from the original definition.

471 **C.1 (Global) MANTEL Test**

472 Given the Euclidean distance matrices \tilde{A} and \tilde{B} , the MANTEL coefficient [8] is defined as

$$\text{Mantel}(X, Y) = \frac{\sum_{i \neq j}^n (a_{ij} - \bar{a})(b_{ij} - \bar{b})}{\sqrt{\sum_{i \neq j}^n (a_{ij} - \bar{a})^2 \sum_{i \neq j}^n (b_{ij} - \bar{b})^2}}, \quad (1)$$

473 where $A = \tilde{A}$, $B = \tilde{B}$, $\bar{a} = \frac{1}{n(n-1)} \sum_{i \neq j}^n (a_{ij})$ and similarly for \bar{b} . Then the MANTEL test is carried out
 474 by the permutation test.

475 Unlike distance correlation and H_{HG}, the MANTEL test is not consistent against all dependent alter-
 476 natives, but it has been a very popular method in biology and ecology due to its simplicity. It is
 477 clear from Figure A3 and A4 that global MANTEL is sub-optimal and appears to be not consistent

478 for many dependencies, yet MGC_P achieves comparable performances as other variants of MGC ,
 479 which implies that MGC_P may be consistent against most, if not all dependent alternatives.

480 C.2 (Global) Distance Correlation

481 Given two distance matrices \tilde{A} and \tilde{B} of the sample data X and Y , the sample distance covariance
 482 is defined by doubly centering the distance matrices:

$$dcov(X, Y) = \frac{1}{n^2} \sum_{i,j=1}^n a_{ij} b_{ij}, \quad (2)$$

where $A = H\tilde{A}H$, $B = H\tilde{B}H$ with $H = I_n - \frac{J_n}{n}$. Then the sample distance variance is defined as

$$\begin{aligned} dvar(X) &= \frac{1}{n^2} \sum_{i,j=1}^n a_{ij}^2, \\ dvar(Y) &= \frac{1}{n^2} \sum_{i,j=1}^n b_{ij}^2, \end{aligned}$$

483 and the sample distance correlation equals

$$\text{Dcorr}(X, Y) = \frac{dcov(X)}{\sqrt{dvar(X) \cdot dvar(Y)}}. \quad (3)$$

484 It is shown in [9] that as $n \rightarrow \infty$, $\text{Dcorr}(X, Y) \rightarrow \text{Dcorr}(x, y) \geq 0$, where $\text{Dcorr}(x, y)$ denotes
 485 the population distance correlation between the underlying random variable x and y . The pop-
 486 ulation distance correlation is defined by the characteristic functions, which is 0 if and only if x
 487 and y are independent. Thus the sample distance correlation is a consistent statistic for testing
 488 independence, i.e., the testing power $\beta_\alpha(\text{Dcorr}(X, Y))$ converges to 1 as n increases, at any type
 489 1 error level α . Note that all of $dcov$, $dvar$, Dcorr are always non-negative; and the consistency
 490 result assumes finite second moments of x and y , which holds for a family of metrics not limited
 491 to the Euclidean distance [11]. Also note that the Dcorr above is actually the square of distance
 492 correlation in [9], but for ease of presentation the square naming is dropped here.

493 Alternatively, calculating the distance covariance by $A = H\tilde{A}$ and $B = \tilde{B}H$ gives the same statis-
 494 tic as in Equation 2, i.e., instead of using doubly centered distance matrices, it is the same to
 495 singly center one distance matrix by row and the other distance matrix by column. Then Dcorr by
 496 singly centered distance matrices has the same testing power as the original Dcorr , because dis-
 497 tance covariance is equivalent to distance correlation in the permutation test (note that the actual

498 D_{corr} statistic by single centering is different from the original D_{corr}, as using single centering
 499 changes the distance variances).

500 In our implementation of global / local D_{corr}, we always use singly centered distance matrices
 501 rather than doubly centered distance matrices. Although they are equivalent for the testing power
 502 of global D_{corr}, our alternative implementation improves the testing power of local D_{corr} and
 503 M_{gc}. This is because the ranking information of \tilde{A} and \tilde{B} are better preserved in singly centered
 504 distance matrices, so that M_{gc} is more effective in excluding far-away points that exhibit insignificant
 505 dependency. This applies to M_{corr} as well.

506 C.3 (Global) Modified Distance Correlation

507 In case of high-dimensional data where the dimension d_x or d_y increases with the sample size n ,
 508 the sample distance correlation may no longer be appropriate. For example, even for independent
 509 Gaussian distributions, D_{corr}(X, Y) $\rightarrow 1$ as $d_x, d_y \rightarrow \infty$, which may severely impair the testing
 510 power of sample D_{corr} in high-dimensional simulations.

511 The modified distance correlation is proposed in [10] to tackle the bias of sample D_{corr}. Denote
 512 the Euclidean distance matrices as \tilde{A} and \tilde{B} , the doubly centered distance matrices as \hat{A} and \hat{B} ,
 513 the modified distance covariance is defined as

$$mcov(X, Y) = \frac{n}{(n-1)^2(n-3)} \left(\sum_{i \neq j}^n a_{ij} b_{ij} - \frac{2}{n-2} \sum_{j=1}^n a_{jj} b_{jj} \right), \quad (4)$$

514 where A modifies the entries of \hat{A} by

$$a_{ij} = \begin{cases} \hat{a}_{ij} - \frac{\tilde{a}_{ij}}{n}, & \text{if } i \neq j, \\ \frac{n \sum_i \tilde{a}_{ij} - \sum_{i,j} \tilde{a}_{ij}}{n^2}, & \text{if } i = j, \end{cases}$$

515 and so is B . Then mvar(X) and mvar(Y) can be similarly defined.

516 If mvar(X) \cdot mvar(Y) ≤ 0 , the modified distance correlation is set to 0 (negativity can only occur
 517 when $n \leq 2$, equality can only happen in some special cases); otherwise it is defined as

$$Mcorr(X, Y) = \frac{mcov(X, Y)}{\sqrt{mvar(X) \cdot mvar(Y)}}. \quad (5)$$

518 It is shown in [10] that M_{corr}(X, Y) is an unbiased estimator of the population distance correlation
 519 D_{corr}(x, y) for all d_x, d_y, n ; and M_{corr} is approximately normal even if $d_x, d_y \rightarrow \infty$. Thus it is a

520 consistent statistic for testing independence, but may work better than DCORR under high-dimension
521 dependencies.

522 Similar to the alternative implementation of DCORR , we can also use singly centered distance ma-
523 trices for \hat{A} and \hat{B} in defining MCORR , which does not alter the theoretical advantages of original
524 MCORR . We further set $A_{ii} = B_{ii} = 0$ for all i , which simplifies the expression of MCORR and is
525 asymptotically equivalent for the testing purpose.

526 C.4 Multiscale Graph Correlations (MGC)

527 For any generalized correlation coefficient, its local correlations can be directly implemented as
528 in Equation 3, by plugging in the respective a_{ij} and b_{ij} from Equation 1 and sorting the distance
529 matrices column-wise as in Equation 2.

530 In particular, MANTEL sets a_{ij} and b_{ij} as the respective entry of \tilde{A} and \tilde{B} (the Euclidean distances).
531 DCORR lets a_{ij} and b_{ij} be the respective matrix entry of A and B (the doubly centered distance
532 matrices), then the sample means \bar{a}, \bar{b} are automatically 0. MCORR slightly modifies a_{ij} and b_{ij} of
533 DCORR to adjust their high-dimensional bias. As discussed already, our version of MGC_M is based
534 on single centering throughout: we take $a_{ij} = b_{ij} = 0$ when $i = j$, otherwise set a_{ij} as the matrix
535 entry of $H\tilde{A} - \tilde{A}/n$, and set b_{ij} as the entry of $\tilde{B}H - \tilde{B}/n$. Then the local version of MCORR follows
536 by Equation 3.

537 Generally, there are a total of $\max(R(a_{ij})) \times \max(R(b_{ij}))$ local correlations, which equals n^2 when
538 there exists no repeating data. Note that we use minimal ranks in sorting when ties occur, which
539 indexes all local correlations more conveniently than breaking ties randomly or using average /
540 max ranks.

541 Among all possible local correlations, MGC picks the optimal local correlation that yields the best
542 testing power. The optimal scale clearly exists, but is distribution dependent and is almost always
543 non-unique. Among all local correlations, it suffices to exclude C^{1l} and C^{k1} for testing and optimal
544 scale estimation: since $C^{1l} = C^{k1} = C^{11}$, they do not include any neighbor other than each obser-
545 vation itself, merely count the diagonal terms in the distance matrices, and are not meaningful for
546 the testing purpose.

547 **C.5 Heller, Heller & Gorfine (HHG)**

548 The HHG statistic applies Pearson's chi-square test to ranks of distances within each column, and is
 549 shown to be better than many global tests including DCORR under common nonlinear dependencies
 550 in [27, 28]. Like DCORR and MCORR , HHG is distance-based and consistent, but not in the form of the
 551 generalized correlation coefficient; and like our MGC , it makes use of the rank information, but in a
 552 distinct manner.

Given the Euclidean distance matrices $\tilde{A} = [\tilde{a}_{ij}]$ and $\tilde{B} = [\tilde{b}_{ij}]$, we denote

$$\begin{aligned} H_{11}(i, j) &= \sum_{q=1, q \neq i, j}^n I(\tilde{a}_{ik} \leq \tilde{a}_{ij}) I(\tilde{b}_{ik} \leq \tilde{b}_{ij}) \\ H_{12}(i, j) &= \sum_{q=1, q \neq i, j}^n I(\tilde{a}_{ik} \leq \tilde{a}_{ij}) I(\tilde{b}_{ik} > \tilde{b}_{ij}) \\ H_{21}(i, j) &= \sum_{q=1, q \neq i, j}^n I(\tilde{a}_{ik} > \tilde{a}_{ij}) I(\tilde{b}_{ik} \leq \tilde{b}_{ij}) \\ H_{22}(i, j) &= \sum_{q=1, q \neq i, j}^n I(\tilde{a}_{ik} > \tilde{a}_{ij}) I(\tilde{b}_{ik} > \tilde{b}_{ij}), \end{aligned}$$

and the HHG statistic is defined as

$$\text{HHg}(X, Y) = \sum_{i=1, j \neq i}^n \frac{(n-2)(H_{12}(i, j)H_{21}(i, j) - H_{11}(i, j)H_{22}(i, j))^2}{H_{1\cdot}(i, j)H_{2\cdot}(i, j) - H_{1\cdot}(i, j)H_{2\cdot}(i, j)},$$

553 where $H_{1\cdot} = H_{11} + H_{12}$, $H_{2\cdot} = H_{21} + H_{22}$, $H_{1\cdot} = H_{11} + H_{21}$, and $H_{2\cdot} = H_{12} + H_{22}$. It is clear
 554 that HHG is structurally different from DCORR / MCORR / MANTEL , cannot be conveniently expressed by
 555 Equation 1, and there is no direct extension of local correlation to HHG .

556 The permutation test using the HHG statistic is consistent against all dependent alternatives. In
 557 our numerical simulations, HHG falls a bit short when testing against high-dimensional and noisy
 558 linear dependencies, but is often more advantageous than global correlations under nonlinear
 559 dependencies, which makes it a strong competitor in general.

560 **D MGC Algorithms and Testing Procedures**

561 In this section we elaborate on the algorithms for computing local correlation and MGC , as well as
 562 their testing procedures in simulations and real data experiment.

563 Five algorithms are presented in section D.1: given the choice of a global correlation coefficient,
564 algorithm 1 computes one local correlation coefficient at a given (k, l) ; then algorithm 2 shows
565 how to compute all local correlations simultaneously; algorithm 3 computes the p-values of all
566 local correlation by the random permutation test; algorithm 4 approximates the optimal scale for
567 Mgc based on the p-values of all local correlations, and outputs the approximated p-value of Mgc;
568 algorithm 5 estimates the testing powers of all local statistics based on a given joint distribution
569 or multiple pairs of data, which can be used to more accurately estimate the optimal scale for
570 Mgc when the underlying model is known or training data are given. More detailed discussions
571 regarding the optimal scale approximation is offered in section D.2.

572 D.1 Algorithms

573 All algorithms are implemented in Matlab and R with the pseudo-code shown below. For ease of
574 presentation, we assume there are no repeating data and take Dcorr as the global correlation in
575 the pseudo-code.

576 Algorithm 1 shows a straightforward computation of one local correlation coefficient, which re-
577 quires $O(n^2)$ once the rank information is provided. This is suitable for Mgc computation when
578 the optimal local scale is known or already estimated. But using algorithm 1 to compute all local
579 correlations would require iterating through all possible neighborhoods (k, l) , which takes $O(n^4)$
580 and would make the optimal scale estimation computationally inefficient.

581 To facilitate the optimal scale estimation, algorithm 2 provides a fast method to compute all lo-
582 cal correlations in $O(n^2)$. An important observation is that each product $a_{ij}b_{ij}$ is included in C^{kl}
583 if and only if (k, l) satisfies $k \leq R(a_{ij})$ and $l \leq R(b_{ij})$, so it suffices to iterate through $a_{ij}b_{ij}$ for
584 $i, j = 1, \dots, n$, and add the product simultaneously to all C^{kl} whose scales are no more than
585 $(R(a_{ij}), R(b_{ij}))$. However, accessing and adding multiple C^{kl} at the same time is not computa-
586 tionally efficient; instead, for each product, we only add it to C^{kl} at $(k, l) = (R(a_{ij}), R(b_{ij}))$ (so only one
587 local scale is accessed for each operation), iterate through all products for $i, j = 1, \dots, n$, then add
588 up adjacent C^{kl} for $k, l = 1, \dots, n$. Thus all local correlations can be computed in $O(n^2)$, which
589 has the same running time complexity as the global distance correlation. There are two additional
590 overheads: sorting the distance matrices column-wise takes $O(n^2 \log n)$, and properly centering
591 the distance matrices takes $O(n^2)$.

592 Algorithm 3 computes the p-values of all local correlation by the permutation test with r random

593 permutations, which takes $O(rn^2 \log n)$.

594 Algorithm 4 approximates the optimal scale (k^*, l^*) from the p-values of all local correlations,
595 and outputs the approximated Mgc p-value. This is necessary for testing on one pair of data
596 with unknown model, while algorithm 5 is more appropriate for known model. Conceptually, the
597 algorithm first searches for a set of “valid” adjacent rows $\mathcal{K} = \{k_1, k_1 + 1, \dots, k_2 - 1, k_2\}$ such that
598 the median p-value of $\{p_{kl}, k \in \mathcal{K}, l = 2, \dots, n\}$ is no larger than $\alpha/(n-1) * |\mathcal{K}|$, otherwise we take
599 $\mathcal{K} = \{n\}$; and similarly determine the set of valid columns \mathcal{L} . Once \mathcal{K} and \mathcal{L} are determined, the
600 optimal scale (k^*, l^*) is found by the scale that minimizes the p-value within $\{p_{kl}, k \in \mathcal{K}, l \in \mathcal{L}\}$.
601 Clearly if the majority p-values of all local correlations are less than α , then $\mathcal{K} = \mathcal{L} = \{1, \dots, n\}$,
602 and the optimal scale equals the scale that minimizes the p-values among all local correlations;
603 if there is no valid rows and columns, then Mgc takes the largest scale and equals the global
604 correlation. Note that the actual algorithm is a simpler version of the above description: instead of
605 considering all possible sets of rows and check the validity, we limit the check to the most likely set
606 of rows, by first looking for the row scale of the smallest p-value, then including all adjacent rows
607 whose minimal p-value on the row is no larger than α ; similarly for the set of columns.

608 Algorithm 5 computes the testing powers of all local correlations by repeated simulating samples
609 generated from the joint distribution f_{xy} . Sample data under the null and the alternative are re-
610 peatedly generated for r Monte-Carlo replicates, and algorithm 2 is applied to compute the sample
611 local correlations under the null and the alternative. Then the testing power at each local corre-
612 lation can be estimated, and the Mgc optimal scale can be found by maximizing the powers. This
613 algorithm is also applicable if there exists multiple pairs of data with unknown model but similar
614 dependency structure, then the alternative statistic can be computed from each data pair while
615 the null statistic can be computed from each data pair under permutation. The running time is
616 $O(rn^2 \log n)$.

617 D.2 Discussions of Optimal Scale Estimation

618 To evaluate Mgc in simulations or real data, the optimal scale for Mgc always needs to be estimated
619 first. Algorithm 5 computes the testing powers of all local correlations for known model, so the
620 optimal scale (k^*, l^*) can be directly estimated by maximizing the testing powers (if there are more
621 than one optimal scales, one may pick the scale that maximizes the mean difference of the test
622 statistic under the null and the alternative). Once the optimal scale is determined, the testing

Algorithm 1 Local Correlation Computation for One Scale

Input: A pair of distance matrices $(\tilde{A}, \tilde{B}) \in \mathbb{R}^{n \times n} \times \mathbb{R}^{n \times n}$, and the given local scale $(k, l) \in \mathbb{R} \times \mathbb{R}$.
Output: The local correlation coefficient $C^{kl} \in [-1, 1]$ at the given (k, l) .

```
1: function LOCALCORR( $\tilde{A}, \tilde{B}, k, l$ )
2:   initialize  $C^{kl}, V_k^A, V_l^B, E_k^A, E_l^B$  as 0.
3:   for  $Z := A, B$  do  $R^Z = \text{SORT}(\tilde{Z})$  end for            $\triangleright$  column-wise sorting and assume no ties
4:   for  $Z := A, B$  do  $Z = \text{CENTER}(\tilde{Z})$  end for        $\triangleright$  proper centering of the distance matrices
5:   for  $i, j = 1, \dots, n$  do
6:      $C^{kl} = C^{kl} + A_{ij}B_{ij}\mathbf{I}(R_{ij}^A \leq k)\mathbf{I}(R_{ij}^B \leq l)$            $\triangleright$  store local distance covariance
7:      $V_k^A = V_k^A + A_{ij}^2\mathbf{I}(R_{ij}^A \leq k)$            $\triangleright$  store local distance variance for  $X$ 
8:      $V_l^B = V_l^B + B_{ij}^2\mathbf{I}(R_{ij}^B \leq l)$            $\triangleright$  store local distance variance for  $Y$ 
9:      $E_k^A = E_k^A + A_{ij}\mathbf{I}(R_{ij}^A \leq k)$            $\triangleright$  store the sample means
10:     $E_l^B = E_l^B + B_{ij}\mathbf{I}(R_{ij}^B \leq l)$ 
11:   end for
12:    $C^{kl} = (C^{kl} - E_k^A E_l^B / n^2) / \sqrt{(V_k^A - E_k^{A2} / n^2)(V_l^B - E_l^{B2} / n^2)}$        $\triangleright$  normalize the local covariances
13: end function
```

Algorithm 2 $O(n^2 \log n)$ Algorithm for Computing All Local Correlations

Input: A pair of distance matrices $(\tilde{A}, \tilde{B}) \in \mathbb{R}^{n \times n} \times \mathbb{R}^{n \times n}$.
Output: All local correlation coefficients $C^{kl} \in [-1, 1]^{n \times n}$ for $k, l = 1, \dots, n$.

```

1: function LOCALCORR( $\tilde{A}, \tilde{B}$ )
2:   initialize  $C$  as a zero matrix of size  $n \times n$ ;  $V^A, V^B, E^A, E^B$  as zero vectors of size  $n$ .
3:   for  $Z := A, B$  do  $R^Z = \text{SORT}(\tilde{Z})$  end for
4:   for  $Z := A, B$  do  $Z = \text{CENTER}(\tilde{Z})$  end for
5:   for  $i, j = 1, \dots, n$  do
6:      $k = R_{ij}^A$ 
7:      $l = R_{ij}^B$ 
8:      $C^{kl} = C^{kl} + A_{ij}B_{ij}$ 
9:      $V_k^A = V_k^A + A_{ij}^2$ 
10:     $V_l^B = V_l^B + B_{ij}^2$ 
11:     $E_k^A = E_k^A + A_{ij}$ 
12:     $E_l^B = E_l^B + B_{ij}$ 
13:   end for
      ▷ the next two for loops with respect to the scales guarantee the computation of all local
      covariance / variance in  $O(n^2)$ 
14:   for  $k = 1, \dots, n - 1$  do
15:      $C^{1,k+1} = C^{1,k} + C^{1,k+1}$ 
16:      $C^{k+1,1} = C^{k+1,1} + C^{k+1,1}$ 
17:     for  $Z := A, B$  do  $V_{k+1}^Z = V_k^Z + V_{k+1}^Z$  end for
18:     for  $Z := A, B$  do  $E_{k+1}^Z = E_k^Z + E_{k+1}^Z$  end for
19:   end for
20:   for  $k, l = 1, \dots, n - 1$  do
21:      $C^{k+1,l+1} = C^{k+1,l} + C^{k,l+1} + C^{k+1,l+1} - C^{k,l}$ 
22:   end for
23:   for  $k, l = 1, \dots, n$  do                                ▷ normalize all local covariances
24:      $C^{kl} = (C^{kl} - E_k^A E_l^B / n^2) / \sqrt{(V_k^A - E_k^A)^2 / n^2 (V_l^B - E_l^B)^2 / n^2}$ 
25:   end for
26: end function

```

Algorithm 3 P-value Computation for All Local Correlations

Input: A pair of distance matrices $(\tilde{A}, \tilde{B}) \in \mathbb{R}^{n \times n} \times \mathbb{R}^{n \times n}$, the number of permutations r .
Output: The p-value matrix $P \in [0, 1]^{n \times n}$ for all local distance correlations.

```
1: function PERMUTATIONTEST( $\tilde{A}, \tilde{B}, r$ )
2:    $C^{kl} = \text{LOCALCORR}(\tilde{A}, \tilde{B})$                                  $\triangleright$  calculate the observed local correlations
3:   for  $j = 1, \dots, r$  do
4:      $\pi = \text{RANDPERM}(n)$                                           $\triangleright$  generate a random permutation of size  $n$ 
5:      $C_0^{kl}[j] = \text{LOCALCORR}(\tilde{A}, \tilde{B}(\pi, \pi))$            $\triangleright$  calculate the permuted test statistics
6:   end for
7:   for  $k, l = 1, \dots, n$  do
8:      $P_{kl} = \sum_{j=1}^r (C^{kl} < C_0^{kl}[j]) / r$                    $\triangleright$  get the p-value at each local scale
9:   end for
10:  end function
```

623 power of M_{GC} under the given model can be quickly determined by algorithm 5, and its p-value for
624 testing on a particular pair of data can be determined by algorithm 3.

625 If there is only one pair of data (X, Y) with unknown distributions, we have to approximate the
626 optimal scale by algorithm 4. It makes use of Bonferroni correction to separately verify the set of
627 rows and columns, which guarantees the false positive rate to be no higher than α ; otherwise the
628 scale is set to the largest, which guarantees the approximated M_{GC} is at least as powerful as the
629 global correlation. Still, algorithm 4 is a heuristic approach to approximate the optimal local scale,
630 which does not guarantee the optimal local correlation to be always correctly identified.

631 To better justify algorithm 4, we compare the estimated M_{GC} power by algorithm 4 to the true
632 M_{GC} power by algorithm 5, with the global M_{CORR} and H_{HG} as benchmarks. For each type of depen-
633 dency in the simulation section, we generate 1,000 pairs of dependent data by the same low- and
634 high-dimensional settings as in Figure A4 and A3; and for each pair of data, all local p-values are
635 calculated by 1,000 random permutations. By using the true optimal scale (from the simulation sec-
636 tion) consistently for each data pair, the true M_{GC} p-value can be computed; by using algorithm 4 to
637 approximate the optimal scale for each pair of data separately, the estimated M_{GC} p-value can be
638 computed; and the p-values of global M_{CORR} and H_{HG} can also be derived. The null is rejected when
639 the p-value is less than 0.05, and the power equals the percentage of correct rejection. Based on
640 the powers of true M_{GC} / estimated M_{GC} / M_{CORR} / H_{HG} shown in Figure A2, we observe that although

Algorithm 4 Optimal Local Scale Approximation by P-values

Input: The p-value matrix $P \in \mathbb{R}^{n \times n}$ of all local distance correlations, the type 1 error level α .

Output: The approximated MGC optimal scale (k^*, l^*) , and the approximated MGC p-value p .

```
1: function MGCSCALEVERIFY( $P, \alpha$ )
2:    $\mathcal{K} = \text{VERIFYRow}(P, \alpha)$                                  $\triangleright$  search for a set of valid row indices
3:    $\mathcal{L} = \text{VERIFYRow}(P^T, \alpha)$                              $\triangleright$  search for a set of valid column indices
4:    $[k^*, l^*] = \arg \min_{\{k \in \mathcal{K}, l \in \mathcal{L}\}} P_{kl}$            $\triangleright$  find the optimal scale within the valid range
5:    $p = P_{k^*l^*}$ 
6: end function
```

Input: Same as MGCSCALEVERIFY.

Output: The indices of valid rows.

```
1: function VERIFYRow( $P, \alpha$ )
2:   initialize  $\mathcal{K}$  as an empty set
3:    $[k^*, l^*] = \arg \min_{k,l} \{P_{kl}, k, l = 2, \dots, n\}$ 
4:   for  $k = k^*, \dots, 2$  do                                 $\triangleright$  check all row scales no larger than  $k^*$ 
5:     if  $\min\{P_{kl}, l = 2, \dots, n\} > \alpha$  then
6:       break
7:     end if
8:      $\mathcal{K} = [k, \mathcal{K}]$ 
9:   end for
10:  for  $k = k^* + 1, \dots, m$  do                       $\triangleright$  check all row scales larger than  $k^*$ 
11:    if  $\min\{P_{kl}, l = 2, \dots, n\} > \alpha$  then
12:      break
13:    end if
14:     $\mathcal{K} = \{\mathcal{K}, k\}$ 
15:  end for
16:  if  $\text{MEDIAN}(P_{kl}, k \in \mathcal{K}, l = 2, \dots, n) > \alpha * \frac{|\mathcal{K}|}{n-1}$  then
17:     $\mathcal{K} = \{n\}$             $\triangleright$  take the largest scale if the median p-value is not sufficiently small
18:  end if
19: end function
```

Algorithm 5 Testing Powers Computation for All Local Correlations

Input: A joint distribution f_{xy} , the sample size n , the number of MC replicates r , and the type 1 error level α .

Output: The power matrix $\beta_\alpha \in [0,1]^{n \times n}$ for all local correlations, and the Mgc optimal scale $(k^*, l^*) \in \mathbb{R} \times \mathbb{R}$.

```
1: function TESTINGPOWERS( $f_{xy}, n, r, \alpha$ )
2:   for  $j = 1, \dots, r$  do
3:     for  $i := [n]$  do  $(X_i^1, Y_i^1) \stackrel{iid}{\sim} f_{xy}$  end for            $\triangleright$  generate dependent samples
4:     for  $i := [n]$  do  $X_i^0 \stackrel{iid}{\sim} f_x$  end for                    $\triangleright$  generate independent samples
5:     for  $i := [n]$  do  $Y_i^0 \stackrel{iid}{\sim} f_y$  end for
6:     for  $Z := A, B$  do  $\tilde{Z}_1 = \text{DIST}(Z_1)$  end for     $\triangleright$  the distance matrices under the alternative
7:     for  $Z := A, B$  do  $\tilde{Z}_0 = \text{DIST}(Z_0)$  end for       $\triangleright$  the distance matrices under the null
8:      $C_1^{kl}[j] = \text{LOCALCORR}(\tilde{A}_1, \tilde{B}_1)$         $\triangleright$  calculate all local correlations under the alternative
9:      $C_0^{kl}[j] = \text{LOCALCORR}(\tilde{A}_0, \tilde{B}_0)$         $\triangleright$  calculate all local correlations under the null
10:   end for
11:   for  $k, l = 1, \dots, n$  do
12:      $c_\alpha = \text{CDF}_{1-\alpha}(C_{kl}^0[j], j \in [r])$            $\triangleright$  get the critical value by the empirical cumulative
        distribution under the null at each scale
13:      $\beta_\alpha^{kl} = \sum_{j=1}^r (C_{kl}^1[j] > c_\alpha) / r$             $\triangleright$  estimate the power
14:   end for
15:    $(k^*, l^*) = \arg \max(\beta_\alpha^{kl})$                        $\triangleright$  find the optimal local scale
16: end function
```

641 the estimated MGC power by algorithm 4 can be lower than the true MGC power, it is almost always
642 better than global MCORR and HHG, and combines the better performance of the two benchmarks.

643 Note that it is tempting to directly use the optimal scale that minimizes all local p-values without
644 the validation by algorithm 4, or generate random samples based on the given data pair and use
645 algorithm 5 by bootstrap. However, both approaches are biased such that the false positive rate will
646 be higher than the type 1 error in the absence of dependency. This is because for a given pair of
647 data, a non-optimal scale can happen to have a significant p-value, which may be falsely identified
648 as optimal if we directly minimize all local p-values. Those erroneous scales often still exist after
649 a straightforward re-sampling, so random samples have the same problem. More investigations
650 into the bias and better methods for searching the optimal scale are two worthwhile directions for
651 future works.

652 E Proofs

653 **Theorem 1.** $\beta(C_t^*) \rightarrow 1$ for all f_{xy} in \mathcal{F}_t .

654 *Proof.* For any f_{xy} , the power of multiscale graph correlation satisfies

$$\beta(C^*) = \max_{\mathbf{x}, k, l} \{\beta(C^{kl})\} \geq \beta(C), \quad (6)$$

655 at any type 1 error level α . So $\beta(C^*) \rightarrow 1$ if $\beta(C) \rightarrow 1$.

656 Therefore $\beta(C_t^*) \rightarrow 1$ for all f_{xy} in \mathcal{F}_t . In particular, MGC_D and MGC_M are consistent against all alter-
657 native of finite second moments, because DCORR and MCORR are consistent against all alternatives
658 of finite second moments by [9, 10]. \square

659 **Theorem 2.** If x is linearly dependent on y , then for any n it always holds that

$$\beta(C^{mn}) = \beta(C^*) = \beta(C). \quad (7)$$

660 Thus the optimal scale for MGC is the global scale for linearly dependent data.

661 *Proof.* To show that MGC is equivalent to the global correlation coefficient, it suffices to show the
662 p-value of C^{kl} is always no less than the p-value of C for all k, l under linear dependence.

663 Under linear dependency, for any global correlation coefficient satisfying Equation 1, by Cauchy-
 664 Schwarz inequality it follows that

$$1 = C(X, Y) \geq C(X, YQ) \quad (8)$$

665 for any permutation matrix Q , where the equality holds if and only if X is a scalar multiple of YQ .

666 It follows that the p-value of C is 0, which is at the minimal.

667 Therefore the p-value of C^{kl} cannot be less than the p-value of C under linear dependency, such
 668 that the global correlation is the optimal scale for MGC under linear dependency. \square

669 **Theorem 3.** *There exists f_{xy} and n such that*

$$\beta(C^*) > \beta(C). \quad (9)$$

670 *Thus multiscale graph correlation can be better than its global correlation coefficient under certain
 671 nonlinear dependency, for finite sample.*

672 *Proof.* We give a simple discrete example of f_{xy} at $n = 7$, such that the p-value of MGC_M is strictly
 673 lower than the p-value of MCORR .

Suppose under the alternative, each pair of observation (x, y) is sampled as follows:

$$\begin{aligned} x &\in \{-1, -\frac{2}{3}, -\frac{1}{3}, 0, \frac{1}{3}, \frac{2}{3}, 1\} \text{ without replacement,} \\ y &= x^2, \end{aligned}$$

674 which is a discrete version of the quadratic relationship in the simulations.

675 At $n = 7$, we can directly calculate $C^{kl}(X, Y)$ and $\{C^{kl}(X, YQ)\}$ for all permutation matrices Q . It
 676 follows that the p-value of MCORR is $\frac{151}{210}$, while $C^{kl}(X, Y) = \frac{17}{70}$ at $(k, l) = (2, 4)$. Note that in this
 677 case k is bounded above by $n = 7$ while l is bounded above by 4 due to the repeating points in
 678 Y .

679 Then by choosing $\alpha = 0.25$, MGC has power 1 while global MCORR has power 0, i.e., MGC successfully
 680 identifies the dependency in this example while global MCORR fails.

681 Note that we can always consider sample points in $[-1, 1]$ for X , increase n and reach the same
 682 conclusion with more significant p-values; but the computation of all possible permuted test statis-
 683 tics becomes more time-consuming as n increases. The same conclusion also holds for MGC_D and
 684 MGC_P using the same example. \square